

Progress of polysaccharide-based tissue adhesives

Gi-Yeon Han^a, Ho-Wook Kwack^a, Yo-Han Kim^b, Yeon Ho Je^b, Hyun-Joong Kim^{a,*}, Chong-Su Cho^{b,*}

^a Program in Environmental Materials Science, Department of Agriculture, Forestry and Bioresources, Seoul National University, Seoul 08826, Republic of Korea

^b Department of Agricultural Biotechnology, Research Institute of Agriculture and Life Sciences, Seoul National University, Seoul 08826, Republic of Korea

ARTICLE INFO

Keywords:

Tissue adhesive
Natural polymer
Polysaccharide
Next-generation

ABSTRACT

Recently, polymer-based tissue adhesives (TAs) have gained the attention of scientists and industries as alternatives to sutures for sealing and closing wounds or incisions because of their ease of use, low cost, minimal tissue damage, and short application time. However, poor mechanical properties and weak adhesion strength limit the application of TAs, although numerous studies have attempted to develop new TAs with enhanced performance. Therefore, next-generation TAs with improved multifunctional properties are required. In this review, we address the requirements of polymeric TAs, adhesive characteristics, adhesion strength assessment methods, adhesion mechanisms, applications, advantages and disadvantages, and commercial products of polysaccharide (PS)-based TAs, including chitosan (CS), alginate (AL), dextran (DE), and hyaluronic acid (HA). Additionally, future perspectives are discussed.

1. Introduction

Every year, more than million people in the world experience various wounds due to traumatic incidents, surgical incisions, and diabetic ulcers (Steiner, Karaca, Moore, Imshaug, & Pickens, 2017). Traditionally, invasive techniques such as sutures, staples, clips, and skin closure strips are the gold standard for wound closure and they stop bleeding, prevent leakage, and restore tissue structure and function. Among them, absorbable sutures having a flexibility with mechanical features and simplified use, have been used to suture deeper wounds without the need for removal following wound healing while non-absorbable sutures have been used to close superficial wounds (Bal-Ozturk et al., 2021). However, this option has several limitations, such as infection risk, granuloma formation, lengthy process, anesthesia requirement, and skilled by trained personnel requirement (Su, Wei, Dai, Zhang, & Xia, 2019). Therefore, the use of tissue adhesives (TAs) has attracted the attention of scientists and industry because of several advantages, such as blood leakage prevention, less pain, less surgery time, infection mitigation, non-requirement for removal procedures, and minimally invasive surgery (Scognamiglio et al., 2016).

Polymeric TAs composed of natural or synthetic polymers can provide multiple functions owing to the generation of three-dimensional networks for binding to the target tissue (Scognamiglio et al., 2016). Natural polymeric TAs include protein-based TAs, such as fibrin,

albumin, and gelatin. Polysaccharide (PS)-based TAs include chitosan (CS), alginate (AL), dextran (DE), and hyaluronic acid (HA). Starch-based hemostatic materials have a low adhesive ability because they are easily washed away if pressure is not exerted during application. Additionally, preparing cellulose-based TAs is not easy due to their insolubility in water and most organic solvents. The CS-based TAs have several advantages, such as biocompatibility, biodegradability, antibacterial activity, and applicability in various formulations and chemical modifications. It should be noted that the source of the CS affects the physicochemical and biological properties due to its biological origin, molecular weight, and degree of acetylation. The AL-based TAs have several advantages, such as biocompatibility, wound healing, good injectability, low toxicity, and good swelling behavior, although AL is non-degradable in the body and ionically cross-linked AL can be easily dissolved in water. Additionally, the source of AL affects physicochemical properties. The DE-based TAs have several advantages, such as biocompatibility, degradability, injectability, and low toxicity, although the degradation rate of oxidized-DE TA is relatively fast owing to the hydrolysis of imine bonds. The HA-based TAs have several advantages, such as the property of being a natural moisturizer with a high water-binding capacity due to its highly hydrophilic nature, biocompatibility, biodegradability, non-immunogenicity, and angiogenesis. However, they exhibit poor mechanical properties owing to their high swelling and rapid degradation. On the other hand, synthetic TAs, such

* Corresponding authors.

E-mail addresses: hjokim@snu.ac.kr (H.-J. Kim), choes@snu.ac.kr (C.-S. Cho).

<https://doi.org/10.1016/j.carbpol.2023.121634>

Received 22 September 2023; Received in revised form 20 November 2023; Accepted 21 November 2023

Available online 28 November 2023

0144-8617/© 2023 Elsevier Ltd. All rights reserved.

as polycyanoacrylate (PCA), poly(ethylene glycol) (PEG), and polyurethane (PU), exhibit high adhesive strength and low biocompatibility.

Recent review articles on tissue adhesives can be categorized under various topics. First is the source of the polymer, e.g., from PS and PS/protein among natural polymers and natural/synthetic polymers. Shokrani et al. addressed the chemistry of PS-based tissue adhesives in terms of the mechanisms underlying the tissue adhesiveness (Shokrani et al., 2022). Montazerian et al. discussed the natural polymers of proteins and PS design for developing tough adhesive surgical sealants and methods to get toughness and adhesion in regard to natural polymers (Montazerian et al., 2022). Li et al. focused on clinical translations and natural polymer-based bioadhesives (Li et al., 2022a). Bao et al. discussed design strategies and adhesive mechanisms for the natural- and synthetic-based tissue adhesives (Bao, Gao, Sun, Nian, & Xian, 2020). Nam et al. addressed tissue-targeted adhesives using natural and synthetic polymers in terms of the chemistry and biology of the tissue (Nam & Mooney, 2021). Bal-Ozturk et al. focused on natural and synthetic polymer-based tissue adhesives from research to clinical translation (Bal-Ozturk et al., 2021). The second category is functional tissue adhesives, including monofunctionality and multifunctionality. Among the monofunctional polymer-based tissue adhesives, O'Rorke et al. discussed UV bioadhesives as activated bioadhesives because they allow when and where a bioadhesive crosslinks and the extent of the crosslinking by a UV irradiation (O'Rorke et al., 2017). Bhagat et al. discussed degradable tissue adhesives because current commercial- or clinical-approved tissue adhesives were limited due to their lack of degradability (Bhagat & Becker, 2017). Park et al. addressed functional bioadhesives which enhanced tissue healing and effective biosignal sensing and their use for the practical applications (Park, Kim, Chun, & Seo, 2021). Erdi et al. addressed polymer nanomaterials for use as adjuvant surgical tools to overcome the shortcomings of reduced mechanical stability and the inability of adherence to complex tissue surfaces (Erdi, Sandler, & Kofinas, 2023). Recently, Bertsch et al. provided the current state of self-healing injectable hydrogels for various tissue regenerations and the bioprinting of complex tissue constructs (Bertsch, Diba, Mooney, & Leeuwenburgh, 2022). In a different vein, Pinnaratip et al. discussed multifunctional bioadhesives categorized as passive and active by design (Pinnaratip, Bhuiyan, Meyers, Rajachar, & Lee, 2019). The passive ones contain inherent compositions and structural designs for antimicrobial properties, self-healing ability, and the promotion of cellular ingrowth, whereas the active ones respond to stimuli changes such as pH, temperature, light electricity and biomolecular concentration. The third category is tissue adhesives for targeted tissues. Musculoskeletal tissue, including bone, intervertebral disc, articular cartilage, knee meniscus, and tendon caused by injuries or degenerative diseases (Tarafder, Park, Felix, & Lee, 2020), oral wounds during dental and surgical procedures using cyanoacrylate (Borie et al., 2019), ocular tissues caused by an accident or surgery using synthetic or naturally derived polymeric adhesives (Trujillo-de Santiago et al., 2019). Additionally, surgical adhesives for neuro-surgery, orthopedic, periodontal, ophthalmic, cardiovascular, pneumothoracic, gastrointestinal, plastic, and reconstructive surgeries using natural polymers (Jain & Wairkar, 2019), and bone fracture healing using synthetic or natural polymers were discussed.

In this review, we discuss the requirements of polymeric TAs, mechanisms of adhesion, adhesion testing methods, adhesive assessment techniques, applications of adhesives, advantages/disadvantages, and commercial products of PS-based TAs. Additionally, future perspectives are discussed.

2. Requirements of polymeric TAs

Ideal TAs should have certain properties (Scognamiglio et al., 2016): First, they should be non-local irritants, anti-inflammatory, non-toxic, and non-antigenic. Second, they should be easily applied to target tissues. Third, they must be biodegradable after performing their

functions. Fourth, reticulation should occur in body fluids. Fifth, pliability should be similar to that of the target tissue for expansion/contraction under physiological conditions. Sixth, they should have a strong binding ability to obtain adequate mechanical properties. Finally, adhesion bonding should be maintained under wet physiological conditions. However, clinically used TAs meet only a few requirements because the appropriate TA for a specific selection should meet the required properties according to the specific target tissues.

3. Mechanisms of adhesion

Adhesion is a bonding process between two distinct. In fundamental terms, adhesion occurs when there is van der Waals forces between the adhesives and substrates. Moreover, other physical, chemical, and biological interactions can affect the adhesion. In this chapter, the mechanisms and influencing factors of tissue adhesive are discussed.

3.1. Physical mechanisms

The physical intermolecular interactions are important for initial adhesion. Among the physical interactions, hydrogen bonding, van der Waals forces, and electrostatic interactions are the basic interactions that affect the adhesion. These interactions can simply be induced by introducing polar functional groups. Moreover, the adhesion can occur direct interactions such as mechanical interlocking and chain entanglement. We will discuss the physical mechanisms in more detail.

3.1.1. Hydrogen bonding and electrostatic interactions

Hydrogen bond interaction between a proton donor species and a proton acceptor can be occurred. Catechol and gallol have two and three hydroxyl groups at the benzene ring, respectively, and these hydroxyl groups can form hydrogen bonds. Therefore, adhesives containing many catechol and gallol groups exhibit high adhesion due to a large number of hydroxyl groups. Electrostatic interactions occur between the oppositely charged molecules. Electrostatic interactions are most easily observed among polar molecules, which contain a carboxylic acid and amine groups. Cui et al. fabricated a dopamine hyper-branched polymer as an injectable adhesive. Through hydrophobic association and the hydrogen bonding of dopamine, a hyper-branched polymer was produced in-situ gelation under wet conditions, and it exhibited a high adhesion with diver polymeric surfaces and tissues (Cui et al., 2019). Zhao et al. fabricated biocomponent adhesives based on lysine-rich recombinant proteins. They fabricated lysin-rich engineered protein (LEP) adhesive through the crosslinking between lysine-rich protein, glutaraldehyde (GA) and oxidized hyaluronic acid (OHA). LEP exhibited high tissue adhesion due to the hydrogen bonds and electrostatic bonds between amine groups in lysine and tissue surface, and carboxylic acid groups in the OHA (Fig. 1a) (Zhao et al., 2023). Choi et al. constructed a densely assembled network hydrogel using green tea extracts such as epigallocatechin gallate (EGCG) and catechin. Through the dynamic and reversible hydrogen bonding, the hydrogel exhibited a high tissue adhesion with strain-tolerance (Choi, Kang, Son, & Shin, 2022). Electrostatic interactions occurred between the oppositely charged molecules. Electrostatic interactions are most easily observed among polar molecules, which contain a carboxylic acid and amine groups. Wang et al. reported a tough hydrogel adhesive based on hydrogen bonding and electrostatic interactions. Carboxylic acid and imidazole groups can interact with each other and tissue surface, thereby exhibiting excellent toughness and adhesiveness (Wang et al., 2022d).

3.1.2. Mechanical interlocking

Mechanical interlocking is a method for increasing the adhesion strength by expanding the adhesion surface area. This method can be achieved by wetting the adhesive into the irregularities of a rough surface or patterned surface. Yang et al. introduced a biphasic microneedle with a non-swellaable core and swellaable tip at the adhesive surface for

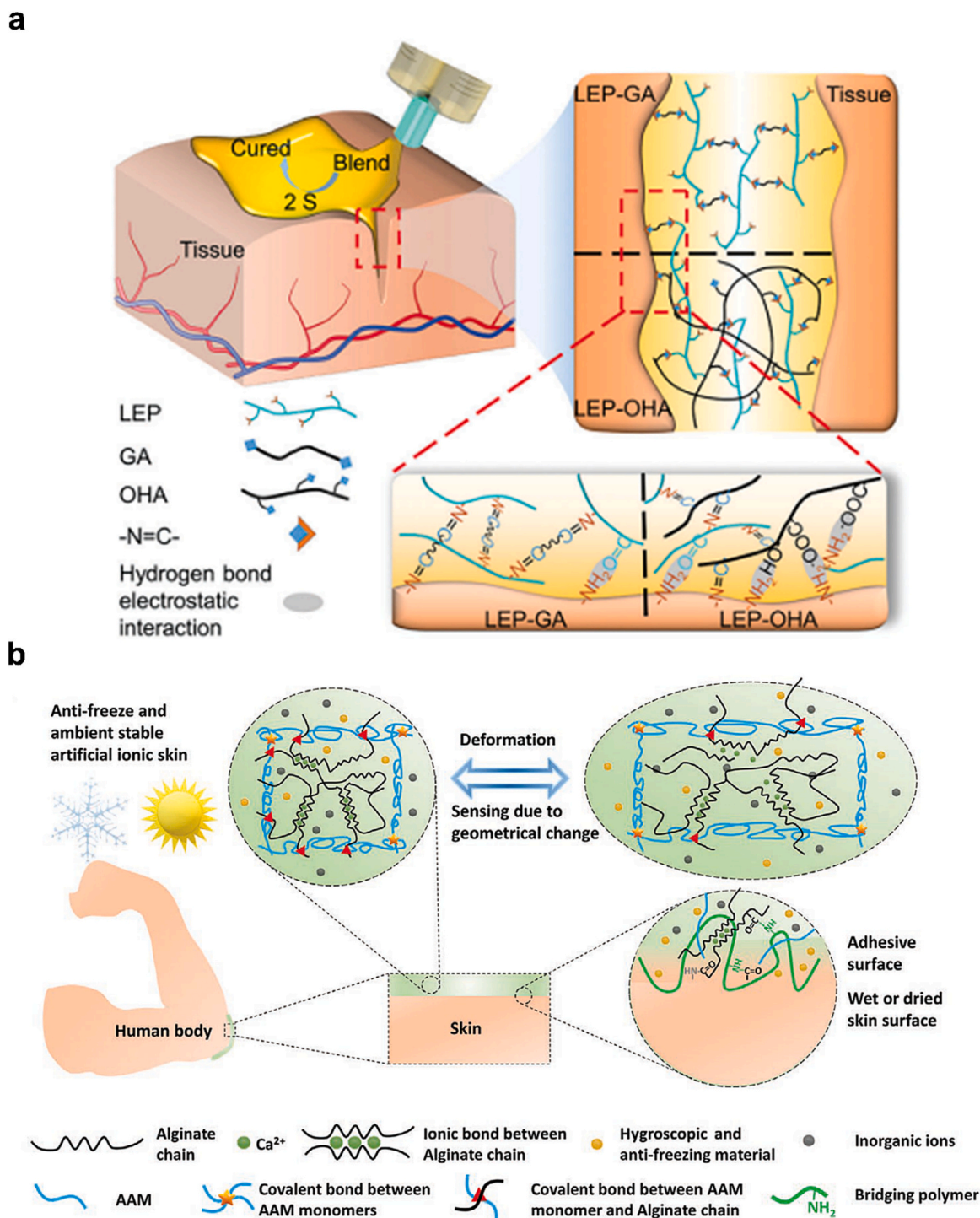


Fig. 1. Mechanism of physical adhesion. a) Hydrogen bond and electrostatic interactions, and b) chain entanglement by bridging polymers. [Adapted from Zhao et al., 2023 and Ying et al., 2021 with permission from John Wiley and Sons.]

mechanical interlocking. By introducing this needle, the adhesive could penetrate the soft tissue surface and this caused swellable tip interlocking with the dermis (Yang et al., 2013).

3.1.3. Chain entanglement

Chain entanglement between dissimilar materials can be formed by the diffusion of polymer chains due to capillary action and electrostatic interactions. Chain diffusion is affected by molecular weight, chain length, and chain concentrations (Shakir, Prashant, Keerti, & K, T. R., & NK, J., 2016). The most widely used diffusive polymer in the biomedical

fields is CS. Ying et al. used CS as a bridging polymer. It can be absorbed by the target surface by electrostatic interactions and then, forming physical entanglements. Through this bridging polymer, their hydrogel exhibited a high adhesion energy with respect to a variety of tissue and polymeric surface (Fig. 1b) (Ying, Chen, Zuo, Li, & Liu, 2021).

3.2. Chemical mechanisms

Chemical crosslinking is stronger than physical interactions and can form robust adhesion between the adhesive and substrate. Chemical

crosslinking reactions are of many types. Among them, amide-based crosslinking reactions are used for tissue adhesives because biological tissue contain a large amount of amide groups. We will discuss the chemical mechanisms in more detail.

3.2.1. Carbodiimide coupling and imine reactions

A carbodiimide coupling reaction occurs between carboxyl and amine groups, and an imine coupling reaction occurs between an aldehyde and amine. Both types of coupling reactions have been widely used. Cintron-Cruz et al. achieved additional tissue adhesion strength by carbodiimide coupling reactions of CS. They performed the robust adhesion through carbodiimide reaction between topologically entangled CS and AL adherend (Cintron-Cruz et al., 2022). Wu et al. incorporated *N*-hydroxysuccinimide (NHS) ester groups in adhesive, and the NHS ester group formed covalent bonds by a carbodiimide reaction. Therefore, they exhibited robust and long-term stable tissue adhesiveness (Fig. 2a) (Wu, Yuk, Wu, Nabzdyk, & Zhao, 2021). Ma et al. introduced *o*-nitrobenzene in CS to fabricate photo-responsive hydrogel adhesives. Under UV irradiation, *o*-nitrobenzene converted to *o*-nitrobenzylaldehyde, and the aldehyde group formed crosslinks with the amine groups of CS and the tissue surface by an imine reaction (Fig. 2b) (Ma et al., 2020).

3.2.2. Michael addition reaction

The Michael addition reaction occurs between a vinyl group and an amine or thiol group. This reaction has been easily observed in catechol chemistry. When a dopamine molecule is oxidized to the quinone form, amine or thiol can form a covalent bond through the Michael coupling reaction (Salazar, Martín, & González-Mora, 2016). Moreover, this reaction is used for crosslinking bioadhesives. Shin et al. grafted dopamine on CS for use as the sealing and hemostatic agent. The grafted dopamine molecules formed crosslinks with the amine groups of CS and the tissue. They suggested that the dopamine-grafted film exhibited a self-sealing property (Shin et al., 2017).

3.2.3. Surface treatments

The facile way to form covalent bonds between an adhesive and substrate is the surface functionalization of the substrate. By introducing reactive functionalized groups on the substrate, interaction between the adhesive and substrate can dramatically increased. Tian et al. introduced 3-(trimethoxysilyl)propylmethacrylate, triethoxyvinylsilane to a hydrophilic polyacrylamide hydrogel and polydimethylsiloxane hydrophobic elastomer, respectively. Through the coupling reaction agents, strong interfacial bonding between dissimilar materials was achieved (Tian, Suo, & Vlassak, 2020). Moreover, Li et al. treated a metal surface with 12-methacrylamidododecanoic acid through a simple drop-casting. Carboxyl groups can bind to a metal ion through electrostatic and hydrophobic interactions, and they achieved a tough adhesion through copolymerization with methacrylate groups and with a hydrogel precursor (Li et al., 2019). These coupling agents formed an adhesion between organic and inorganic materials through their reactive functional groups.

3.3. Biological mechanism

Various interactions between biomolecules and biomolecules during metabolic process of organisms are possible mechanisms for tissue adhesion (Shokrani et al., 2022). The tissue adhesion can occur under mild conditions without any specific pH and temperature. Among the typical examples of tissue adhesion with biological mechanisms are thrombin–fibrinogen, avidin–biotin interactions, and disulfide bonds involved in protein–protein interactions. We will discuss the biological mechanisms in more detail.

3.3.1. Thrombin–fibrinogen interaction

Generally, blood coagulation is initiated by a clotting cascade after

injury, and it is divided into two cascades (Wang et al., 2022a). The primary hemostasis ends with the formation of a platelet plug, which is accompanied by a release of clotting substances and adsorption, activation, and aggregation of platelets. Subsequently, the secondary hemostasis process starts with the activation of the intrinsic and extrinsic coagulation pathways. In this process, thrombin induces the conversion of fibrinogen to fibrin, which forms a firm clot in the presence of coagulation factor FXIII. Also, the fibrin adhesive comprise fibrinogen, thrombin, factor XIII, and Ca^{2+} was approved by the FDA in 1998 (Nam & Mooney, 2021).

3.3.2. Avidin–biotin interaction

The avidin–biotin bond has been applied in several applications, such as immunoassays, diagnostics, chromatography, drug delivery, cell culture, and tissue engineering (Tsai & Wang, 2005). This is because avidin as a tetrameric glycoprotein, exists in egg whites has a specific and strong interaction with biotin molecules (dissociation constant of $10^{15}/\text{M}$) (Wilchek & Bayer, 1990). Frati et al. developed a novel cardiac patch based on a blend of AL and gelatin designed to improve suture resistance with an effective insulin-like growth factor-1 immobilization using the avidin–biotin technique (Frati et al., 2020).

3.3.3. Disulfide bond

The formation of disulfide bonds during protein–protein interactions is very critical in the initial folding, refolding, regulation of biological function, and the stabilization of proteins (Adams, 2023), although multi-disulfide bonds affect water solubility and protein denaturation. Lu et al. developed antibacterial and biodegradable tissue nano-adhesives for rapid wound closure using disulfide bond-bridged nano-silver-decorated mesoporous silica nanoparticles (Lu et al., 2018). Additionally, Singh et al. prepared thiolated hydroxypropyl methylcellulose phthalate microparticles for the higher uptake of antigens in ileum due to the mucoadhesive property of the carrier. This was suggested through the disulfide bonds formed between the thiol groups in the microparticles as an antigen carrier and cysteine-rich glycoproteins of the mucus layer (Fig. 3) (Singh et al., 2015).

4. Adhesion testing methods

Before introducing the adhesion testing methods, factors that affect the adhesion strength of a TA have to be considered. The most important factor to consider is the water present in the substrate and adhesive. The water layer at the substrate reduces the adhesion strength by interfering with the direct interaction between the adhesive and substrate. If the adhesive absorbs water or retains water itself (in the case of a hydrogel), the adhesion mechanism can be varied depending on the water content and chemical composition of adhesive. From a surface energy perspective, hydrogel adhesives exhibit a difference when compared to that of dry adhesives due to the water in the matrix (Zhang et al., 2020). The work of an adhesion (ω) of dry adhesive can be expressed in Eq. (1).

$$\omega = \gamma_{\text{adhesive}} + \gamma_{\text{adhesive}} - \gamma_{\text{interface}} \quad (1)$$

where γ represents the surface energy.

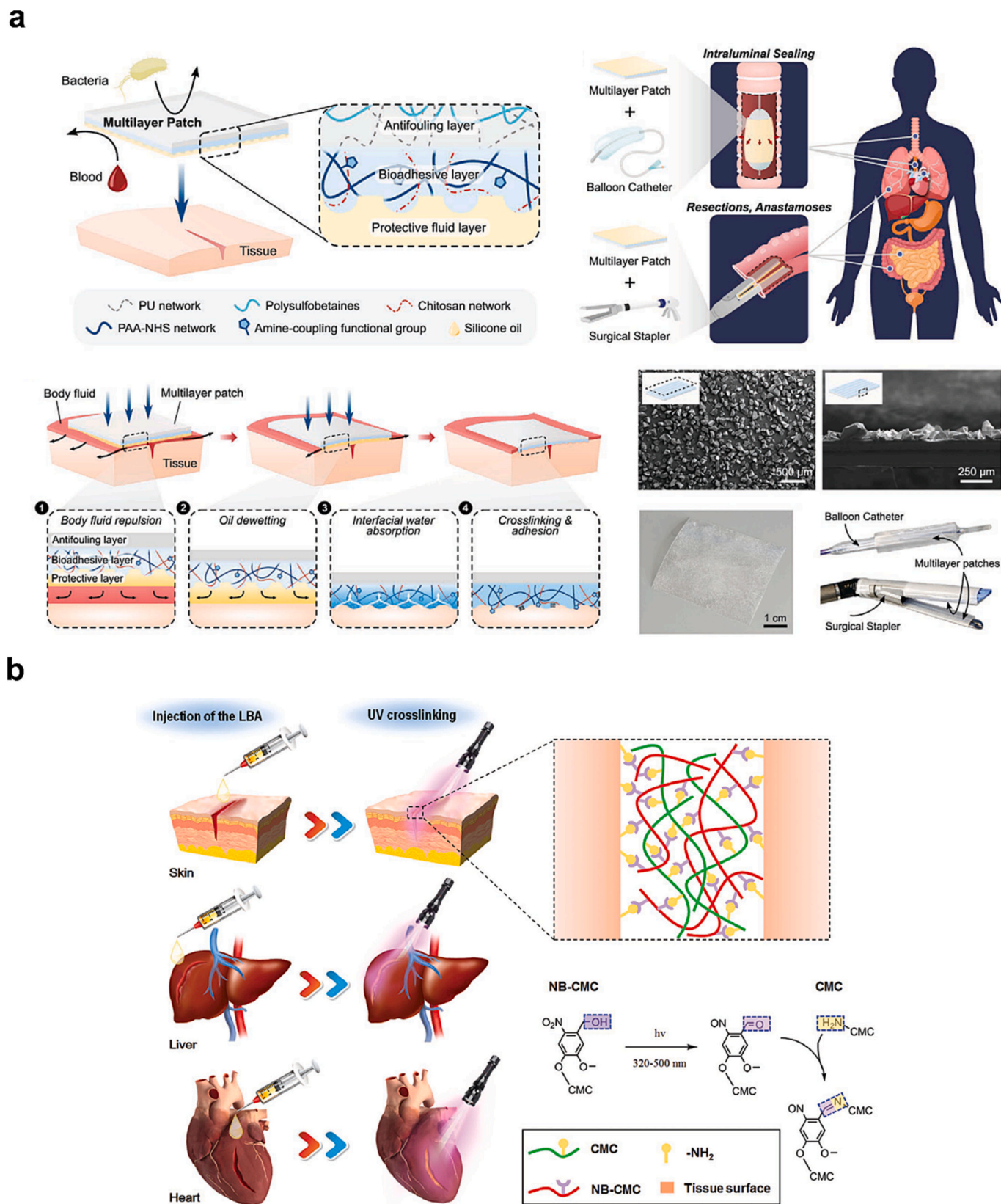
The surface energies of the adhesives differ because of their water intake capacities. The work of adhesion of the hydrogel adhesive can be expressed using Eqs. (2) and (3):

$$\omega = \gamma_{\text{hydrogel}} + \gamma_{\text{substrate}} - \gamma_{\text{interface}} \quad (2)$$

$$\gamma_{\text{hydrogel}} = \Phi_s \gamma_{\text{network}} - (1 - \Phi_s) \gamma_{\text{water}} \quad (3)$$

where Φ_s represents the polymer content of the gel.

As shown in Eq. (3), the water content of the hydrogel significantly affects adhesion. When a hydrogel matrix intakes a significant amount of water ($\Phi_s \approx 0$), the surface energy of hydrogel is similar to the surface energy of water (i.e., $\gamma_{\text{hydrogel}} \approx \gamma_{\text{water}}$). Therefore, for measuring



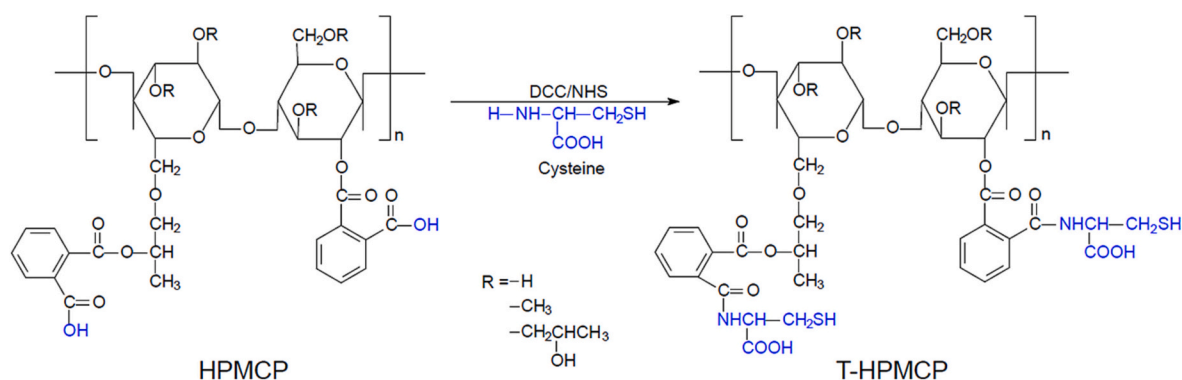


Fig. 3. Schematic synthesis process of thiolated hydroxypropyl methyl cellulose phthalate microparticles. [Adapted from Singh et al., 2015 with permission from Elsevier.]

accurate adhesion strength, strict control of the testing environment, such as humidity or temperature is required.

4.1. Peel test

The peel test is a basic adhesion strength evaluation method that measures the force when the adhesive is peeled off (detached) (Fig. 4a). The peel test was divided into T, 90°, and 180° peels, according to the peeling angle of the adhesive. During the peeling of adhesives, the peeling angle affects the peeling strength, including the size and mechanical properties of the adhesives. These factors were confirmed using Kendall's peel test model (Fig. 5) (Kendall, 1975).

$$\text{Peeling Force} = \left(\frac{F}{b}\right)^2 \frac{1}{2dE} + \frac{F}{b} (1 - \cos\theta) \quad (4)$$

As shown in Eq. (4), the peeling angle and elastic modulus affect the peel strength of the adhesives.

4.2. Tack test

The tack test measures the contact force of the adhesive. The tack test is classified into ball, loop, and probe tacks depending on the measuring apparatus; probe tacks with cylindrical probes are commonly used. A probe-tack test was used to measure the force when the probe was separated from the adhesive (Fig. 4b). Compared with peel and lap shear tests, tack tests are less affected by external factors. The bulk properties

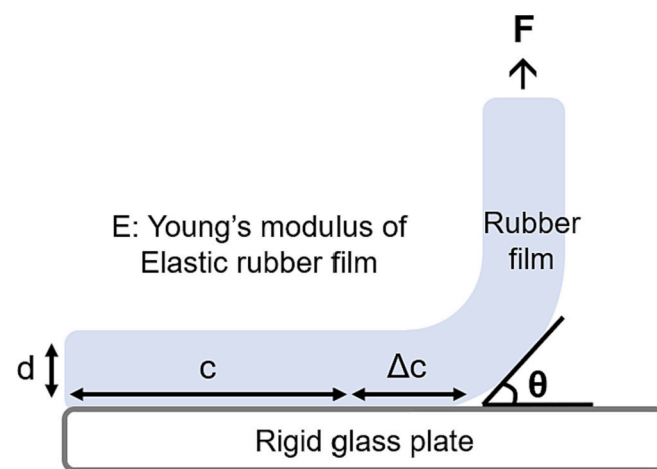


Fig. 5. Kendall's peel test model.

and surface energies of the adhesives affect their tack strengths. These factors were confirmed by using the Kendall model (Kendall, 1975).

$$\text{Tack force} = \sqrt{\frac{8\pi}{(1-\nu^2)} E\omega a^3} \quad (5)$$

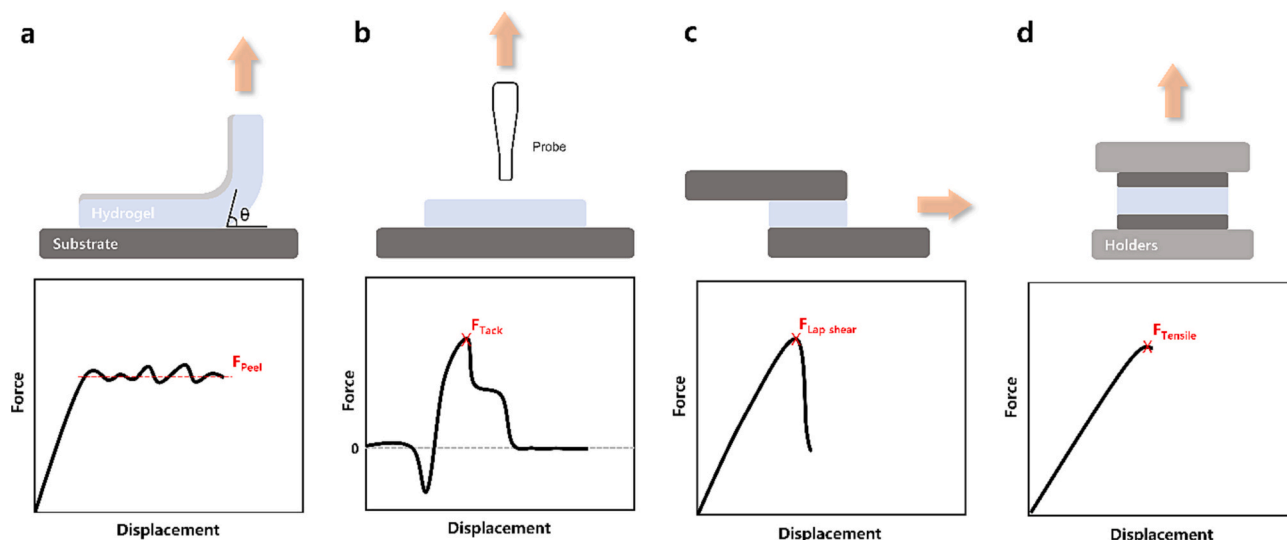


Fig. 4. Schematic illustration of adhesion strength measuring methods. a) Peel, b) probe tack, c) lap shear, and d) tensile tests.

where ν , E , ω , a represent Poisson's ratio of adhesive, Young's modulus of adhesive, surface energy, and adhesion area, respectively.

4.3. Lap shear test

The lap shear test measures the force applied parallel to the adhesion plane when two adhered substrates move in opposite directions (Fig. 4c). The adhesive can withstand the highest stress in the lap shear mode. Lap-shear strength provides long-term maintenance in structural bonding materials and resistance to tissue tension in biomedical applications. However, diverse external factors, such as the sample thickness and elasticity of the substrate, affect the lap shear strength (Suh, Gent, & Kelly, 2007; Wang, Yang, Nian, & Suo, 2020).

4.4. Tensile test

The tensile test measures the force when two adhered substrates stretch in the direction perpendicular to the adhesive surface (Fig. 4d). The tensile test is commonly referred to as a pull-off test. The tensile test can evaluate the amount of force required to separate at the interface of the adhesive and adherend, that is to measure the ability of the adhesive to resist failure. In the tensile test method, the thickness of the substrate greatly affects the tensile strength of the adhesive (Lee, Wang, & Yeo, 2013).

4.5. Other tests

Surface forces apparatus (SFA) is an effective device that can

measure the force between two surfaces as a function of distance (Fig. 6a). Lu et al. used SFA to measure the force of cationic- π interactions in an aqueous solution (Lu et al., 2013). Tang et al. developed an experimental method to determine the debonding energy of highly stretchable materials (Fig. 6b). First, two highly stretchable materials with a small unbonded area were laminated. Second, the critical force at which debonding occurs when the laminated bilayer is pulled can be recorded as the debonding energy (Tang, Li, Vlassak, & Suo, 2016).

5. Adhesive assessments

5.1. Physical assessments

Adhesion strength is the force required to separate the adhesive and adherend, and is a combination of the cohesive and adhesive forces of adhesives. Cohesion is the mechanical strength of the material, and adhesion is the degree of intermolecular interactions that occur at the interface of the adhesive and adherend. The mechanical strength of the adhesive, that is, cohesion, is determined by crosslinking, entanglement, and intermolecular interactions in the polymer network. The mechanical strength (toughness and Young's modulus) of the adhesive was measured through a uniaxial tensile test using a universal testing machine, and the modulus at a specific temperature was measured using a dynamic mechanical analyzer and rheometer. Adhesion is induced by intermolecular interactions occurring at the interface between the adhesive and adherend; physical interactions such as mechanical interlocking and chain diffusion; and chemical interactions such as van der Waals forces, covalent bonds, hydrogen bonds, and ionic bonds. The

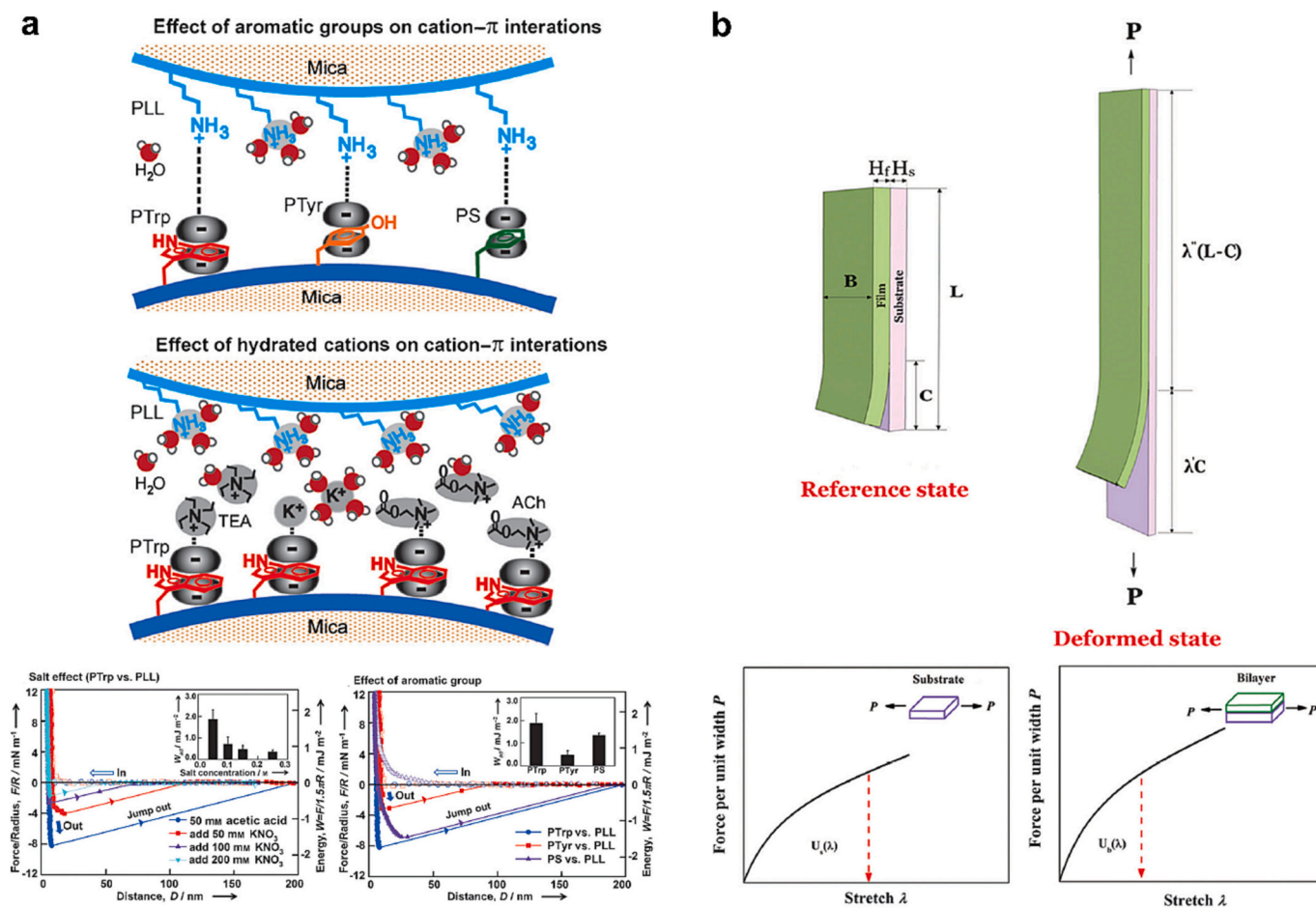


Fig. 6. Adhesion strength measurement using a) surface forces apparatus and b) bilayer debonding test.

[Adapted from Lu et al., 2013 with permission from John Wiley and Sons, and (Tang et al., 2016) with permission from Royal Society of Chemistry.]

adhesive strength was measured using peel and lap shear tests. Notably, owing to the strong intermolecular interactions at the interface, high adhesion strength cannot be achieved. Appropriate cohesion is required to firmly hold the adhesive and adherend upon mechanical stress application. However, if the cohesion is too high, the wettability of the adhesive is reduced, and the adhesion strength decreases (Tobing & Klein, 2001).

Recently, hydrogel adhesives have been used as wound-healing patches in the biomedical field (Pinnaratip et al., 2019). Therefore, hydrogel adhesives should exhibit a high wetting adhesion and water stability (Han, Hwang, Cho, Kim, & Cho, 2023). The human body contains a large amount of water, and organs are surrounded by a wet environment. A wet environment has a water layer on the surface, which hinders direct contact with the adhesive (Zhang et al., 2020). Moreover, the human body has various movable parts, such as the knees and ankles. Therefore, high mechanical resilience and fracture toughness are required to withstand the dynamic environment of the human body. Mechanical resilience, which is the ability of a material to return to its original form when the applied stress is removed, was evaluated using cyclic tensile and compression tests (Zhao et al., 2023). Moreover, a burst pressure test was conducted to confirm its practical application and comprehensively evaluate its mechanical properties (Wang et al., 2023). When hydrogels are applied to a wound site, they require high adhesion to strictly hold tissues and high toughness to withstand the high blood/air pressure and dynamic movement of the human body.

5.2. Chemical assessments

Various chemical analysis techniques have been used to characterize polymeric materials. The most basic methods for tracking polymer reactions are Fourier transform infrared (FT-IR) spectroscopy and nuclear magnetic resonance (NMR) spectroscopy. FT-IR spectroscopy can qualitatively assess the degree of a reaction through the generation or reduction of specific bands during the reaction. Similarly, NMR spectroscopy can be used to determine the degree of reaction. In NMR spectroscopy, a quantitative analysis can be performed by comparing specific peak integrals. Ma et al. confirmed the copolymerization of dopamine methacrylate by FT-IR and NMR (Ma et al., 2018). Furthermore, Han et al. calculate the molecular weight of the synthesized oligomer by the integral of the proton NMR peak (Han, Park, Lee, Yi, & Kim, 2022). Ultraviolet-visible (UV-Vis) spectroscopy is another technique used for the qualitative and quantitative analysis of molecules and compounds. UV-Vis spectroscopy is one of the most commonly used techniques in catechol chemistry to assess the oxidation of the catechol moiety. Detrembleur et al. assessed the degree of dopamine oxidation (catechol to quinone) and calculated the chain end-group retention using UV-Vis spectroscopy (Patil, Falentin-Daudré, Jérôme, & Detrembleur, 2015).

Adhesion occurs at the interface between the adhesive and the substrate. Therefore, analysis of the functional groups on the adhesive surface and their reactivity is important. X-ray photoelectron spectroscopy (XPS) is an effective method for quantitatively analyzing functional groups on adhesive surfaces. Hong et al. investigated the formation of chemical bonds (Schiff base reaction) between biological tissue and hydrogels using XPS (Hong et al., 2019). Furthermore, the reactions of functional groups or diffusive chains can be evaluated using fluorescence. Chen et al. evaluated the reaction of NHS-esters using amine-coupled fluorescent U-beads (Chen, Yuk, Wu, Nabzdyk, & Zhao, 2020). Cintron-Cruz et al. verified the interpenetration of CS chains by grafting them onto fluorescein isothiocyanate (Cintron-Cruz et al., 2022).

5.3. Biological assessments

Hydrogel adhesives degrade under physiological conditions, and their degradation products exhibit no harmful effects on cells. Hydrogel

degradation mechanisms can be categorized as follows: 1) hydrolysis, 2) oxidative degradation, and 3) enzymatic degradation (Lynn, Kyriakides, & Bryant, 2010; Zaaba & Jaafar, 2020). Hydrolysis is a chain scission that occurs when water is added to an ester bond, typically poly(ϵ -caprolactone) or poly(lactide-co-glycolide) degrades due to hydrolysis (Baek, Kim, Son, Choi, & Kim, 2021). Oxidative degradation typically occurs in ether bonds when exposed to reactive oxygen species such as free radicals and peroxides, poly(ethylene oxide), which are degraded by thermal and photo-oxidation (de Sainte Claire, 2009). Enzymatic degradation typically occurs in the biological environment. Various types of enzymes exist, such as proteases, collagenases, hyaluronidases, and lipases, and each type of enzyme cleaves specific sites according to its substrate specificity (Banerjee, Chatterjee, & Madras, 2014). The degradation can be evaluated based on the weight change and swelling of the hydrogel. As the hydrogel chains are cleaved and the crosslinking sites are destroyed, the hydrogel loses weight and swells. Changes in each chain were confirmed by size-exclusion chromatography. Hydrogel degradation can be assessed using chemical methods. Molecules with specific functional groups and structures produced by chain cleavage can be identified using NMR and IR spectroscopy. Cui et al. verified the degradation of polymers by confirming the formation of degradation products using NMR (Cui et al., 2019).

The biocompatibility of the hydrogel was evaluated by an *in vitro* cell toxicity assay using the degradation products of the hydrogel. First, the hydrogel-treated medium was prepared by immersing the hydrogels in the cell culture medium for complete degradation. Second, the cells were cultured in a hydrogel-treated medium and observed at certain time intervals. Fibroblast cell lines are most commonly used to evaluate toxicity because they secrete collagen proteins, which contribute to connecting tissues and are actively expressed in wounded tissues (Werner, Krieg, & Smola, 2007). The potential toxicity of the hydrogel to cells can be evaluated by live/dead cell staining, cell viability, cell cytotoxicity, and cell apoptosis. An *in vivo* method to evaluate the biocompatibility of a hydrogel is to implant a hydrogel at the wound site and observe the histological changes. Hydrogels contain a large amount of water; therefore, they promote wound healing by maintaining a moist environment when implanted at the wound site. Quantitative analysis of the wound size and vessel intensity in wounded tissue is a simple method for evaluating the degree of wound healing. Histological evaluation was performed using hematoxylin and eosin (H&E), Masson's trichrome, and immunohistochemistry (IHC). H&E, Masson's, and IHC staining were used to evaluate the thickness, collagen deposition, and angiogenesis of the regenerated tissue (epidermis and dermis), respectively (Bakhtyar, Jeschke, Herer, Sheikholeslam, & Amini-Nik, 2018; Loh et al., 2018). Furthermore, *in-depth* biological assessments were performed. Proteomic analysis can be used to systematically identify and quantify the complete complement of proteins in cells, tissues, organs, biological fluids, and organisms at specific time points. During cell signaling, numerous enzymes and structural proteins are phosphorylated, methylated, acetylated, glycosylated, oxidized, and nitrosylated. A flow cytometer, as a laser-based device, can be used to analyze millions of cells per second to process labeled cells and to identify and quantify the physical and chemical properties of a population of cells, such as cell viability, cell cytotoxicity, and cell apoptosis. Gene expression analysis can be used to detect the expression of genes encoding cell adhesion molecules using quantitative polymerase chain reaction (qPCR), which amplifies a specific segment of DNA to obtain hundreds of millions of copies within a few hours. Enzyme-linked immunosorbent assay (ELISA) can be used to assess the preparation and treatment of cytokines in blood and tissue samples. Cytokine assays are essential for disease diagnosis and monitoring because cytokines play pivotal roles in the progression or regression of pathological processes and are biomarkers for several diseases. Immunophenotyping can be used to study proteins expressed by cells. This technique is commonly used for basic scientific research and laboratory diagnostics. This can be performed on tissue sections, cell suspensions, etc. It involves the labeling of cells with antibodies directed

against surface proteins on their membranes. By choosing appropriate antibodies, cell differentiation can be accurately determined. The labeled cells were processed using a flow cytometer. The entire procedure can be performed on cells from the blood, bone marrow, or spinal fluid within a few hours. Immunophenotyping is a common flow cytometry test, in which fluorophore-conjugated antibodies are used as probes to stain target cells with high avidity and affinity. This technique allows the rapid and easy phenotyping of each cell in a heterogeneous sample according to the presence or absence of a protein combination.

6. Polysaccharide (PS)-based tissue adhesives (TAs)

PS-based TAs have been attractive as natural polymers because of several advantages, such as biocompatibility, ease of availability, biodegradability, tissue compatibility, sustainability, easy chemical modification, cost-effectiveness, and reproducibility from natural resources (Ju, Lee, Hwang, Cho, & Kim, 2022). Among PS-based TAs, CS, AL, DE, and HA are discussed.

6.1. Chitosan (CS)

6.1.1. Characteristics

CS, obtained from the deacetylation of chitin as a component of the exoskeleton of animals and the cell wall of fungi (Khor & Lim, 2003) has been widely used in numerous biomedical applications such as gene or vaccine delivery carriers (Dev et al., 2010; Kim et al., 2023a; Yi et al., 2005), tissue engineering (Vacanti, 2006), and wound dressing (Lee & Bhang, 2023; Muzzarelli, 2009) due to their biocompatibility, non-toxicity, biodegradability, antibacterial properties, easy chemical modification, and adjustable formulations (Kim et al., 2008). Owing to these properties, CS has gained considerable attention in the application of TAs.

6.1.2. Mechanism of adhesion based on the functional groups in adhesives

6.1.2.1. Photochemical TAs. For TAs, Lu et al. conjugated 3-(4-

hydroxyphenyl) propionic acid (HPP) with glycol chitosan (GC). The HPP-conjugated GC solution can gel immediately after blue light illumination in the presence of a ruthenium complex through photochemically crosslinked covalent dityrosine bonds between the phenolic groups (Lu, Liu, Huang, Huang, & Tsai, 2018).

Ruprai et al. incorporated L-3,4-dihydroxyphenylalanine (L-DOPA) and rose Bengal (RB) as a photosensitizer into a CS solution to make porous TA films for tissue repair (Ruprai et al., 2020). L-DOPA increased the tissue bonding strength, RB-initiated photooxidation, and it increased the crosslinking of the catechol-modified hydrogels after green light irradiation (Sato, Aoyagi, Ebara, & Auzély-Velty, 2017). The mechanisms of TA for porous CS films are processed into two parts, as shown in (Fig. 7): the first is photo-oxidation between singlet oxygen at the tissue interface and the tissue collagen by exposure to green LED light. Then, there is chemical bonding between the tissue collagen and the amino groups of CS through Michael addition and Schiff base reaction. This is followed by polymerization of L-DOPA and crosslinking of the amino groups of CS and tissue collagen radicals by photo-oxidation (Redmond & Kochevar, 2019).

Wei et al. prepared photo-induced TA carboxymethyl chitosan (CMCS)-based hydrogels with antibacterial and antioxidant properties for adhesive hydrogel wound dressings. This was performed through Diels-Alder (DA) reactions between quaternary ammonium (QA)- and hydroxyl benzyl-grafted CMCS (QA/HB-CMCS) and poly(ethylene glycol) (PEG) crosslinkers with *o*-nitrobenzyl (NB) groups (Wei et al., 2022) because the *o*-nitrobenzyl groups have a photo-responsive property. The QA/HB-CMCS/NB-PEG hydrogel was prepared through DA reactions between QA/HB-CMCS and NB-PEG within approximately 20 min. The TA was applied to the porcine skin using UV (365 nm) irradiation for 10 min to obtain an adhesive strength through photogenerated *o*-nitrobenzaldehyde by Schiff base-crosslinking between aldehyde and amine groups present in the skin tissues.

6.1.2.2. Catechol (CA)-based TAs. CA-based TAs are of particular interest because in nature mussels secrete CA moiety-rich adhesive proteins and these proteins exhibit strong water-resistant properties.

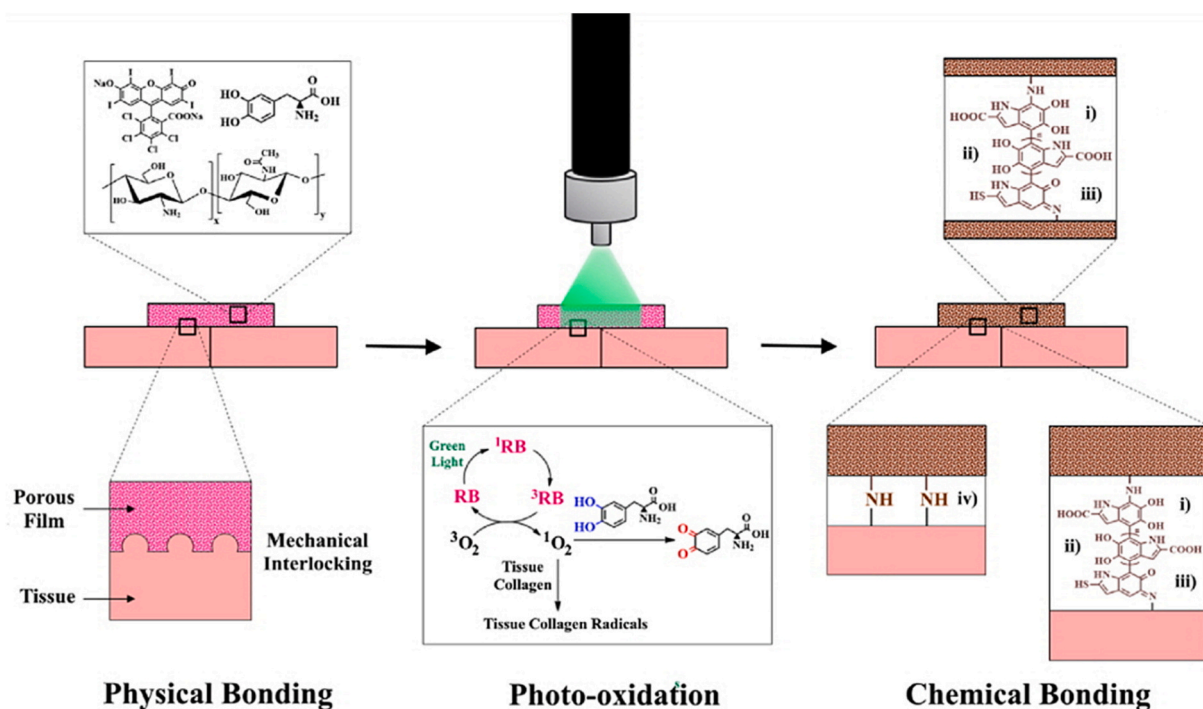


Fig. 7. Possible bonding mechanisms for the CS and DOPA films on tissue. [Adapted from Ruprai et al., 2020 with permission from Elsevier.]

Peng et al. prepared hydrocaffeic acid (HCA)-grafted hydroxymethyl CS (HECS) hydrogels as water-resistant TAs through carbodiimide coupling and tethered CA-induced periodate-stimulated mono- and double-crosslinking with genipin (Peng et al., 2019).

He et al. prepared CA-based injectable hydrogels composed of CS precursor gelation (GE) for infected wound closure by coupling dopamine (DA)-grafted methacrylated gelatin (DA-g-MAGE) and protocatechuic acid (PA)-grafted-methacrylated CS (PA-g-MACS) using H₂O₂/ascorbic acid as a redox-initiated free radical reaction. This reaction involved the activation of ascorbic acid with H₂O₂ (He et al., 2020). Interestingly, the hydrogel solution rapidly cured at body temperature, with wound closure occurring within 60 s in wet and infected wounded mice.

Song et al. prepared CA-based multifunctional hydrogels for tailored TAs through a freeze-thaw of a 3-(3,4-dihydroxyphenyl) propionic acid (DP)-conjugated CS/poly (vinyl alcohol) (PVA) blend and the addition of silver nanoparticles (NPs) into the DP-conjugated CS/PVA blend (Song et al., 2021). This was performed because the physical DP-conjugated CS/PVA blend gels enabled durable and repeatable adhesiveness due to the limited auto-oxidation of the CA groups of the DP-conjugated CS and the hydrogen bonding between the DP-conjugated CS and PVA enabled the hydrogel to self-heal under a mild stimulation. The addition of silver NPs to the hydrogel enhanced its mechanical strength and antibacterial properties.

Rao et al. prepared CA-based multifunctional hydrogels composed of carboxymethyl CS (CMCS) and polydopamine (PDA) for wound-dressing applications (Rao et al., 2022). This was performed through Schiff base cross-linking and hydrogen bonding between CMCS/PDA and covalently crosslinked poly (acryl amide) (PAAM) networks.

Suneetha et al. prepared multifunctional CMCS-based TA hydrogels composed of CMCS reduced graphene oxide (RGO), PDA and PAM (Suneetha, Zo, Choi, & Han, 2023) for wound healing applications. Polymerization of DA followed by the loading GO and its reduction during AM polymerization to get a homogeneously dispersed PAM structure in CMCS solution. The CMCS is water-soluble with antibacterial properties due to containing amino and carboxyl groups. PDA has strong TA properties due to the presence of CA groups, and RGO provides antibacterial and strong mechanical properties. The hydrogels showed multifunctional properties such as antibacterial, biocompatible, and adhesion strength of 32.6 kPa to porcine skin *ex vivo*. Also, they showed the blood clotting time of 60 s whereas the whole blood clots in 360 s.

Rao et al. similarly prepared multifunctional CMCS-based TA hydrogels composed of CMCS, tannic acid, and PAM (Rao, Uthappa, Kim, & Han, 2023) for wound dressing applications by the polymerization of AM in the presence of CMCS and tannic acid. The functional groups such as carboxyl, amine, and hydroxyl groups in the CMCS and amide groups in the PAM easily interact with the phenol hydroxyl groups in the TA via hydrogen bonding. The hydrogels showed enhanced the antibacterial and antioxidant properties and biocompatibility *in vitro* with adhesion strength of up to 39.8 kPa on porcine skin although they did not perform *in vivo* study.

Wu et al. prepared polyelectrolyte complex (PEC)-based powder TAs composed of low molecular weight (LMW) of CS and PAA for acute control by mixing hemorrhage of LMWCS and PAA solutions (Wu et al., 2023a). The PEC powders obtained by freeze drying formed a gel within 5 s upon hydration with strong mechanical, high antibacterial, and strong adhesion properties. Also, the powder remarkably aggregated blood cells and accelerated blood clotting. Furthermore, the powder significantly decreased blood loss and hemostatic time in hemorrhage model of rat tail, liver and heart injuries due to the creation of robust physical barrier and promotion of blood clot formation on the bleeding sites.

6.1.2.3. *Non-covalent-based TAs.* Recently, Cintron et al. prepared non-

covalent-based CS TAs for rapid and strong non-covalent TAs through a combination of pH-responsive bridging CS chains with a tough double-network hydrogel as a dissipative matrix. This hydrogel was composed of covalently cross-linked PAAM and calcium cross-linked AL, as shown in (Fig. 8) (Cintron-Cruz et al., 2022). TAs generated by covalent bonding with functional groups such as -NH₂ and -COOH can be limited by weak, unstable, and slow adhesion. They suggest that a new adhesion mechanism comes from topological entanglement between the CS chains and the permeable adherents.

6.1.2.4. *Poly (ethylene glycol)(PEG)-graft architecture-based TAs.* Kim et al. prepared TAs with a PEG-graft architecture for tissue sealant applications using *in situ* forming hydrogels through a two-step reaction: the first reaction was to synthesize aldehyde-conjugated PEG between PEG and acetic anhydride, and then to synthesize PEG-grafted CS between the amino groups of CS and the aldehyde groups of aldehyde-conjugated PEG through a Schiff base reaction in the presence of sodium cyanoborohydride. The second reaction is to crosslink PEG-grafted CS with dialdehyde-conjugated PEG. It should be noted that the adhesive properties of the hydrogel were affected by the chain length of PEG crosslinker and grafting degree of PEG in the PEG-grafted CS hydrogels.

6.1.2.5. *Dry double-sided TAs.* Yuk et al. prepared dry double-sided TAs (DSTAs) for the strong adhesion of wet tissues and devices through the crosslinking of CS methacrylate (CSMA) and *N*-hydroxysuccinimide (NHS)-grafted-acrylic acid (AA) using UV irradiation to overcome the several limitations of hydrogel TAs (Yuk et al., 2019). The carboxylic acid groups in the NHS-grafted poly (acrylic acid) (PAA) facilitated the rapid hydration and swelling of the DSTAs and this caused the drying of the wet surfaces of the tissues. Additionally, the carboxylic acid groups in the NHS-grafted PAA formed intermolecular bonds, including H-, electrostatic, and covalent bonds with the tissue surfaces.

6.1.2.6. *Enzymatic-crosslinked TAs.* Jung et al. prepared *in situ* forming CS/PEG hydrogels using an enzymatic crosslinking technique with horseradish peroxidase (HRP) as an enzyme for high TAs. This was performed through the reaction of HPP-grafted CS (HPPCS) and tyramine-conjugated PEG (TPEG) in the presence of HRP and H₂O₂ (Jung, Le Thi, HwangBo, Bae, & Park, 2021). This reaction progressed because the HRP catalyzes cross-linking of phenol derivatives in the presence of H₂O₂ (Douglas et al., 2014) without toxicity or unwanted side effects (Jung et al., 2021).

Berg et al. prepared transglutaminase (TG) factor XIII cross-linked

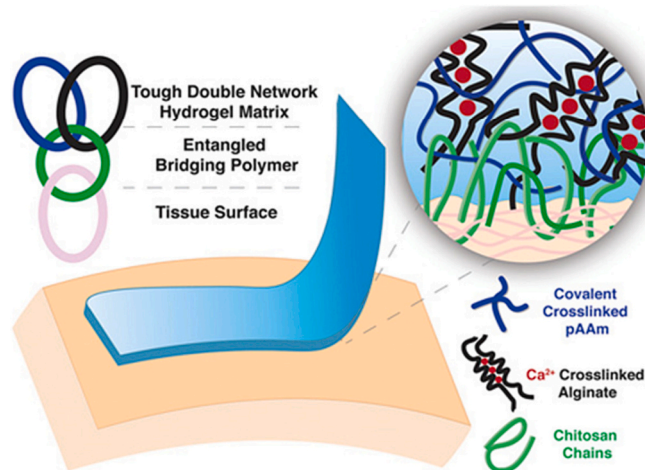


Fig. 8. Schematic of tough double network hydrogel matrix adhered to tissue surfaces.

[Adapted from Cintron-Cruz et al., 2022 with permission from John Wiley and Sons.]

TA CS hydrogels for strong adhesion to cartilage through the reaction of two components: one component was an arginine (AR) or cysteine-containing TQ peptide or reactive lysine-grafted CS; the other was thrombin with Ca^{2+} (Berg et al., 2021). When mixing, thrombin was cleaved to get a fibrin monomer, the fibrin monomers became an unstable fibrin polymer network through hydrogen bonding, and finally, activated factor XIII by thrombin catalyzed chemical cross-linking through amide bonding as well as ionic bonding between cationic CS and anionic tissues, and mechanical interlocking.

6.1.3. Applications

6.1.3.1. Hemostatic agents. Bleeding is the most concerning complication during surgery given its frequent perioperative morbidity.

Park et al. used HCA-grafted GCS as a new hemostatic agent because of the undesired immune response to CA-grafted CS (Park, Lee, Huh, Lee, & Lee, 2019). The results showed that the hemostatic ability of the HCA-grafted GCS was comparable to that of CA-grafted CS with less immune response than CA-grafted CS when treated to the rat liver owing to the antifouling effect of EG groups and reduced adhesion of immune cells; however, the grafting of HCA in the HCA-grafted GCS affected the hemostatic ability, and the tissue adhesiveness was not affected by the EG groups in the HCA-grafted GCS. This is an indication of it being a promising alternative to CA-grafted CS in other biomedical applications.

Sanadiya et al. prepared gallic acid (GA)-conjugated CS for TA and hemostasis because GA has pyrogallol moieties, and tunicates as sea squirts heal the wounded tunic by the oxidization of CA and pyrogallol moieties in tunichrome, forming covalent crosslinking (Sanadiya et al., 2019). The results indicated that GA-conjugated CS hydrogels exhibited greater blood-clotting ability for swine blood than that for CS itself, and the hydrogels exhibited two-fold greater adhesive ability than that of fibrin glue. This is an indication of possibility for a three-dimensional design due to the electrospinning capability.

Li et al. prepared cryogel-type TAs for rapid hemostasis against uncontrollable non-pressing surface hemorrhage through QCS/PDA cryogel network formation obtained by cryopolymerization of QCS and DA in the presence of NaIO_4 as an oxidant because cryogels have strong mechanical strength, stability, and blood absorption properties with strong TA ability (Li et al., 2020b). The cryogels exhibited better hemostasis than gauze in a strip rat liver injury model. This property is an indication of the cryogels being promising candidates for multifunctional TAs.

Han et al. prepared dual biomimetic TA hydrogels based on MACS, DA, and *N*-hydroxymethyl acrylamide (NMA) through a radical polymerization process for sealing hemostasis because MACS and DA imitate the PS intercellular adhesin of staphylococci biofilm and DOPA of mussel foot protein, respectively (Han et al., 2020). The hydrogels exhibited a strong adhesion of 34 kPa even after three cycles of water immersion, with the ability to withstand a blood pressure of up to 168 mmHg. In addition, the hydrogels showed that bleeding in the mouse liver hemorrhage model rapidly stopped within 30 s of treatment with the hydrogels owing to the rapid water-repelling ability and synergistic chemical bonds of MACS and DA at the interface of the liver, whereas PEG diacrylate (PEGDA) hydrogels as the positive control still exhibited bleeding after 120 s. This is an indication of these hydrogels being promising candidates for highly efficient hemostasis and wound healing.

Shou et al. prepared thermoresponsive hydroxybutyl (HB) and CA-grafted CS (HB/CA-CS) hydrogels as an injectable therapeutic approach for hemostasis by grafting HB and CA groups onto the CS backbone, as shown in (Fig. 9) (Shou et al., 2020) because the HB/CA-CS hydrogels have multifunctional properties, such as thermosensitivity, injectability, TA, and wound hemostasis. The hydrogels exhibited sol-gel transitions owing to intramolecular and intermolecular hydrogen bonds and hydrophobic interactions. In addition, the hydrogels still adhered to the chicken bone defect ex vivo under a high-swollen state after being

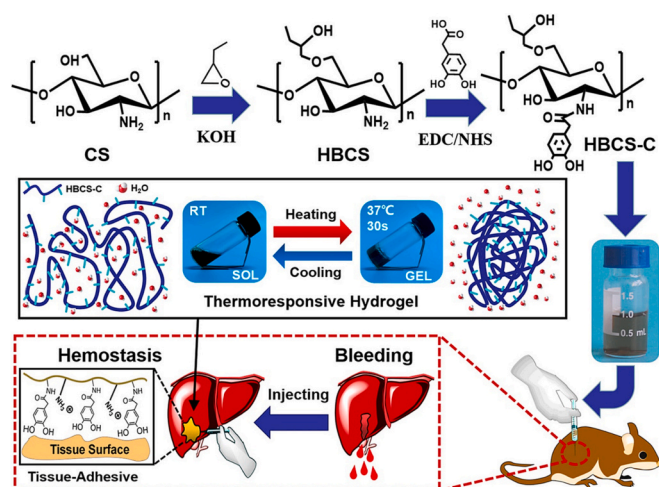


Fig. 9. Schematic illustration of HB/CA-CS thermosensitive adhesive hydrogels.

[Adapted with permission from Shou et al., 2020. Copyright (2020) American Chemical Society.]

immersed in the 0.01 M PBS (pH = 7.4) at 37 °C for 24 h. Furthermore, the hydrogel precursor solution (5 wt.-%) gelled within 30 s after injection in the rat liver model owing to the thermosensitivity of the hydrogels, an indication of serving as an anti-aging barrier stopping wound bleeding, although the bleeding did not completely stop within 30 s. This indicates that these hydrogels being are promising candidates in biomedical applications due to their multifunctional properties.

6.1.3.2. Wound closure. Du et al. prepared multifunctional TAs for sutureless wound closure through the oxidization of HCA-grafted CA dodecyl aldehyde (DA) CS (thus, DACS) lactate composite solutions in the presence of NaIO_4 (Du et al., 2020b) because the sole DACS lactate cannot stop bleeding efficiently because it is easily washed out by the blood flow and has weak mechanical strength of the DACS lactate. The hydrogels exhibited good in situ antibleeding properties with a blood clotting index (BCI) of 7 min in bleeding rat livers, although the BCI depended on the ratio of HCA-grafted CA to DACS lactate. In addition, the hydrogels closed the wound of a rat full-thickness skin incision model within 10 d in a sutureless manner and promoted wound healing compared to the control. This is an indication of these hydrogels being promising candidates for sutureless closure of surgical incisions.

Zheng et al. developed an injectable thermosensitive hydrogel composed of CA-modified quaternary CS (CA-QCS), poly(D,L-lactic acid) (PDLLA)-PEG-PDLLA, and bioactive glass (BG) NPs for wound healing (Zheng et al., 2020). CA-QCS can lower the lower critical solution temperature (LCST) of hydrogels for rapid gelation under physiological conditions and can increase TA, and BG can promote angiogenesis (Chen et al., 2019). The results indicated that the sol-gel transition temperature of the hydrogel was 32.6 °C, which is quite suitable for clinical wound healing although the LCST depended on the concentrations of CA-QCS and BG in the hydrogels. In addition, the hydrogels effectively adhered to the surfaces of various organs, such as the heart, spleen, kidney, and lungs of porcine tissue ex vivo. Furthermore, the hydrogels effectively sealed the skin of ruptured mice, with a significant acceleration of wound healing. This is an indicative of these hydrogels being promising candidates for wound healing through their property of being drug-loaded thermosensitive hydrogels.

Gao et al. developed a hydrogel-mesh composite (HMC) composed of poly (*N*-isopropylacrylamide) (PNIPAM)/CS hydrogels and a poly (ethylene terephthalate) (PET) surgical mesh for wound closure (Gao et al., 2021) to overcome the limitations of the surgical mesh such as stress concentration and tissue damage during surgery. They fabricated

the HMC by soaking a surgical mesh with PNIPAM/CS hydrogel as a precursor because the CS and the tissue formed covalent bonds in the presence of conjugation agent having the adhesion energy of 60–120 J•m⁻² between the HMC and various porcine tissues, and the adhesion was stable due to the LCST of PNIPAM. In addition, the HMC strongly adhered to the wounded tissues of the carotid artery of the sheep, and the large stretch stiffness tightly sealed the wound against blood pressure by bridging a cut under tissue tension. This is indications the potential of the HMC in wound closure on tissues under high pressure or great tension.

Guo et al. have developed injectable hydrogels composed of QCS and tannic acid (TAN) for rapid skin wound healing (Guo et al., 2022a) because QCS has strong TA due to a large number of cations and the formation of ionic bonds with anionic polyphenol groups in TAN, which has several advantages such as antioxidative, anti-inflammatory, and antibacterial properties (Auriemma et al., 2015). The hydrogels rapidly stopped the bleeding of arterial and deep compressive wounds in a mouse tail amputation, with a significant acceleration of wound healing in a full-thickness skin wound model. This is an indication of these hydrogels being promising dressing materials for rapid hemostasis.

Yang et al. developed hybrid TA hydrogel wound dressings composed of CS, PAAM, poly (3-acrylamido phenylboronic acid), and TAN/Fe³⁺ NPs to promote wound healing (Yang et al., 2022) because the hydrogel with free CA, phenylboronic acid, amine, and hydroxyl groups showed high mechanical properties, self-healing ability, and high TA properties owing to the numerous reversible and multiple hydrogen bonds and boronate-ester bonds. The hydrogel showed multifunctional properties such as antibacterial, antioxidant, and anti-inflammatory activities, owing to the embedded TAN/Fe³⁺ NPs in the hydrogel. In addition, the hydrogel effectively prevented biofilm formation and accelerated wound healing at the back of the wound sites in mice. This is an indication of these being potential antibacterial dressings.

6.1.3.3. Bone regeneration. Liu et al. prepared multifunctional bone-adhesive hydrogels composed of CA-modified CS and Zn⁺² ions bridged by imidazolate ligands for bone regeneration (Liu et al., 2020) because the addition of Zn⁺² NPs can stabilize the bone graft environment, promote osteogenic differentiation with blood supply, improve mechanical properties, and accelerate bone reconstruction in CA-modified CS hydrogels. The hydrogels upregulated the production of alkaline phosphatase and osteocalcin and promoted the osteogenic differentiation of rat bone marrow mesenchymal stem cells owing to the release of Zn⁺² NPs from the hydrogels with excellent TA on bovine cortical bone specimens. In addition, the hydrogels promoted vascularized osteogenesis in the wound areas of rats and accelerated the healing of bone reconstruction in a cranial defect rat model. This is an indication of these being promising hydrogels for bone regeneration application.

Fang et al. prepared 3,4-dihydroxy phenyl propionic acid (DP)-grafted CS-based TAs for tendon-to-bone repair (Fang, Linstadt, Genin, Ahn, & Thomopoulos, 2022) because the low adhesion and biocompatibility of DP-grafted CS TA can be overcome by using periodate-modified ion exchange resin filtration to filter off the activating agent and used the resin after oxidation of CA moieties to quinones in the DP-grafted CS. The resulting DP-grafted CS exhibited 6-fold higher adhesion strength in the bovine tendon adhered to bone *ex vivo* compared to commercially available fibrin, with biocompatibility and promotion of tenogenesis *in vitro*, although these were not assessed *in vivo*. This is an indication of potential candidates for tendon-to-bone repair and promotion of healing.

6.1.3.4. Drug delivery system. Chen et al. prepared vascular endothelial growth factor (VEGF)-loaded hybrid hydrogel composed of four-armed benzaldehyde-terminated PEG (BAPEG) and dodecyl-grafted CS (DCS)

through a reversible Schiff base reaction between benzaldehyde and amino groups (Chen et al., 2018) for wound healing because dodecyl tails can insert themselves into and be anchored onto the lipid bilayer of the cell membrane for TA. The hybrid hydrogel exhibited a higher TA ability in the mouse skin defect model with better hemostasis features than the BAPEG/CS hydrogel because of the synergistic effects of covalent bonding between the Schiff base and hydrophobic bonding between the hydrogel and the host cell membranes in the tissues. In addition, the hydrogel significantly improved cell proliferation and tissue remodeling in the wound bed through the controlled release of VEGF from the hybrid hydrogel. This is an indication these hydrogels being promising candidates for wound healing due to their property of being multifunctional drug-loaded hybrid hydrogel.

Moon et al. prepared triclosan (TR)-loaded methacrylate (M)- and succinyl- β -cyclodextrin (CD)-grafted GCS hydrogels by photocrosslinking under visible light irradiation to develop drug-loaded TA (Moon et al., 2021). Because TR is an antibacterial drug, its solubility in water can be improved by a host-guest inclusion complex with MCD-grafted GCS, and water-soluble GCS shows self-healing TA (Du et al., 2020a, 2020b). The resulting hydrogel exhibited two release patterns: an initial burst and sustained release after 48 h *in vitro*. In addition, the hydrogel exhibited improved wound healing on the backs of rats with strong TA compared to fibrin glue. This indicates the potential of these hydrogels in antibacterial tissue adhesives due to the drug-loading ability of the TAs.

Kim et al. prepared 5-fluorouracil (FL)-loaded injectable CS-based TA hydrogels cross-linked by oxidized succinoglycan (OSG) through an aldehyde-amine Schiff-base reaction for wound healing (Kim, Hu, Jeong, & Jung, 2022) because the OSG can be used as a gelling agent with improved mechanical properties and pH-dependent swelling properties (Kim & Jung, 2020). The resulting hydrogels exhibited sufficient adhesive strength of 2763 kPa for wound closure on pig skin, although the adhesion ability of the hydrogels depended on the CS/OSG ratio. In addition, almost 90 % of FL was released from the hydrogel within 48 h at pH 2.0, whereas approximately 60 % of FL was released at pH 7.4, because the network structures of the Schiff bases of CS/OSG collapsed at acidic pH, although they did not perform drug release *in vivo*. This is an indication of these hydrogels being promising candidates for wound healing, tissue engineering, and drug delivery systems due to their multifunctional properties.

Yang et al. prepared compound K (CK)-loaded hydrocaffeic acid-grafted CS TAs for cartilage tissue regeneration (Yang, Shin, Kim, Ryu, & Jin, 2023). TA drug delivery patches to cartilage surfaces can seal cartilage defects and accelerate cartilage regeneration due to CK action as a major metabolite of ginsenosides of protection against joint degeneration. The results showed the prevention of cartilage degradation in osteoarthritis model mice due to the release of CK from the CK-loaded TA patches. This is an indication these CK-loaded TAs being promising candidates for cartilage TA patches.

A list of applications using CS-based TAs is shown in Table 1.

6.1.4. Advantages and disadvantages

CS-based TA has several advantages, such as biocompatibility, biodegradability, antibacterial activity, applicability in various formulations with hydrogels, sponges, and bandages, and various chemical modifications with hydrophilic and hydrophobic groups. However, the physicochemical and biological properties of chitin cannot be precisely controlled because they depend on its biological origin, molecular weight, and degree of acetylation.

6.2. Alginate (AL)

6.2.1. Characteristics

AL obtained from the cell wall of the brown seaweeds consists of α -L-guluronic acid (G-blocks) and β -(1–4)-D-mannuronic acid (M-blocks) as a linear anionic polymer, although the properties of AL are dependent on

Table 1

A list of applications using CS-based TAs.

Category	Main components	In vivo model	Target tissue	Results	Reference
Hemostatic agent	Glycol, chitosan, hydrocaffeic acid	Rat	Liver	Hemostatic ability and less immune responses due to the catechol and glycol groups	(Park et al., 2019)
	Gallic acid, chitosan	Non-treatment	Non-treatment	Strong hemostatic function ability due to the gallic acid	(Sanandiya et al., 2019)
	Polydopamine, quaternized chitosan	Rabbit, mouse	Liver, skin	Excellent hemostatic ability due to the polydopamine	(Li et al., 2020a)
	Methacrylate, dopamine, <i>N</i> -hydroxymethyl acrylamide, chitosan	Mouse, rabbit	Liver, heart	Excellent hemostatic capability due to the biomimetic polymer and dopamine	(Han et al., 2020)
Wound healing	Catechol, hydrobutyl, chitosan	Rat	Liver	Rapid hemostatic ability due to the multiple interactions between catechol/amino groups and tissues	(Shou et al., 2020)
	Hydrocaffeic acid, hydrophobic alkyl chain, chitosan	Rat	Skin	Promotion of wound healing due to good tissue adhesion	(Du et al., 2020a, 2020b)
	Catechol, quaternized chitosan, poly(D,L-lactic acid)-poly(ethylene glycol)-poly(D,L-lactic acid)	Mouse	Skin	Accelerated wound healing due to the loaded bioactive glass	(Zheng et al., 2020)
	Poly(<i>N</i> -isopropylacrylamide), chitosan	Sheep	Carotid artery, lung, liver	Sealing of wounds under tissue tension due to the firm and stable adhesion to tissues	(Gao et al., 2021)
	Tannic acid, quaternary ammonium chitosan	Mouse	Skin	Fast wound healing due to removing of reactive oxygen species by the tannic acid	(Guo et al., 2022a)
	Tannic acid, ferric ion, polyacrylamide, poly(3-acrylamido phenylboronic acid), chitosan	Mouse	Skin	Acceleration of wound healing in infected wounds due to the embedded tannic acid/ferric ion complex	(Yang et al., 2022)
Bone regeneration	Hydrocaffeic acid, zeolitic, imidazole, chitosan,	Rat	Bone	Enhanced bone regeneration due to the zeolite imidazole	(Liu et al., 2020)
	3,4-dihydroxy phenyl chitosan	Non-treatment	Non-treatment	Strong adhesive strength due to the rapid oxidation of 3,4-dihydroxy phenyl moieties by oxidative cross-linking	(Fang et al., 2022; Liu et al., 2020)
Drug delivery system	Benzaldehyde-terminated poly(ethylene glycol), dodecyl-grated chitosan, vascular endothelial growth factor	Mouse	Skin	Outstanding of hemostatic ability due to the released vascular endothelial growth factor	(Chen et al., 2018; Fang et al., 2022)
	Triclosan, beta-cyclodextrin, glycol chitosan	Rat	Skin	Improved wound healing due to the released triclosan	(Chen et al., 2018; Moon et al., 2021)
	5-Fluorouracil, oxidized succinoglycan, chitosan	Non-treatment	Non-treatment	Strong anti-bacterial activity due to the released 5-fluorouracil	(Kim et al., 2022)

(Ju et al., 2022) ratios of M/G blocks. AL has been widely used in biomedical applications such as tissue engineering (Wang et al., 2022c), cell therapy, wound dressing, and drug delivery (Sun, Sun, Xu, & Qian, 2023) systems because AL can be easily formulated into gels, foams, films, fibers, gauze, and wafers (Varaprasad, Jayaramudu, Kanikireddy, Toro, & Sadiku, 2020) and AL is biocompatible, biodegradable, non-toxic, and biostable. Interestingly, AL can be easily cross-linked by binding to divalent metal ions through ionic gelation.

6.2.2. Mechanism of adhesion based on the functional groups present in the adhesives

Pandey et al. prepared mussel-inspired, nanocomposite-based TAs by blending *N*-hydroxysuccinimide-modified poly (lactic-co-glycolic acid) (NHS-PLGA) NPs with dopamine-grafted AL (DOAL) to produce wound-healing TAs (Pandey et al., 2018). NHS-PLGA NPs can increase the properties of the TA through physical adhesive interactions between the NPs and tissue and through chemical bonding between the NHS groups on the NPs and amine groups in the tissue.

Yan et al. prepared mussel-inspired injectable hydrogel-type TAs to develop hemostatic agents by blending hydrazide-modified poly(L-glutamic acid) (HY-PGA) with catechol-and-aldehyde-modified AL (CA/AD-AL) (Yan et al., 2018). This was performed because injectable hydrogels would then be created through the Schiff base reaction between the HY groups in the HY-PGA and the AD groups in the AD-AL, and π - π stacking and hydrogen bonding present between HY-PGA and CA/AD-AL.

Du et al. prepared non-swelling hydrogel TAs composed of Pluronic F127 diacrylate (F127DA), PEGDA, 2-aminoethyl methacrylated AL (AM-AL), and TA for wound closure (Du et al., 2020a). This was performed because the hydrogels could be formed by the free radical polymerization reaction of PEGDA, F127DA, and AM-AL under UV light

in the presence of UV light initiator of Igracure 2959. Additionally, the immersion of TA into the hydrogels increased the storage modulus due to the formation of multiple hydrogen bonds between TA and the hydrogels.

Xing et al. prepared injectable hydrogel TAs composed of oxidized AL (OAL) and adipic acid dihydrazide-modified GE (AD-GE) (Xing et al., 2021). This was performed because the sol-gel transition of the OAL/AD-GE hydrogel could occur quickly through the Schiff base reaction between the amino groups in the AD-GE and the aldehyde groups in the OAL.

Zhang et al. prepared injectable exosome (EX)-loaded hydrogel TAs composed of DO-grafted AL, chondroitin sulfate (CHS), and regenerated silk fibroin (RSF) for endogenous cell recruitment and cartilage defect regeneration (Zhang et al., 2021a). Because DO-grafted AL has strong adhesion ability under wet conditions, CHS has been reported to promote cartilage regeneration (Clegg et al., 2006), and the lysine and tyrosine groups in the RSF enhance adhesion (Lo Presti, Rizzo, Farinola, & Omenetto, 2021).

Toboada et al. prepared sprayable hydrogel TAs composed of oxidized DE (ODE), OAL, and anastomosis polyamidoamine (PAMA) dendrimers for vascular sealing. This was performed because the amine groups in the PAMA dendrimer and aldehyde groups in the ODE and OAL formed imine, hydrogen, and ionic bonds between the tissue and ODE/OAL/PAMA (Munoz Taboada, Dosta, Edelman, & Artzi, 2022).

Wang et al. prepared double network hydrogel TAs composed of a covalently crosslinked primary PNIPAM and a non-covalently cross-linked calcium AL, which resulted in toughness and long-term stability at physiological conditions (Wang et al., 2022b), because the crosslinked PNIPAM hydrogels become hydrophobic due to the LCST of 32 °C (Haq, Su, & Wang, 2017). Additionally, the AL could be non-covalently crosslinked in the presence of calcium ions.

Yao et al. prepared injectable dual-bond cross-linked hydrogel TAs composed of AL, histidine, and Zn^{2+} ions for the efficient healing of infected diabetic wounds (Yao et al., 2022). This was performed because the amine and imidazole groups of histidine could form reversible hydrogen bonds with AL and coordinate bonds with Zn^{2+} ions.

6.2.3. Applications

6.2.3.1. Hemostatic agents. Sunneetha et al. prepared hemostatic hydrogel TAs composed of PDA, AL, and PAAM for skin tissue engineering applications (Sunneetha, Rao, & Han, 2019) because PDA obtained by the alkali-induced polymerization of DA can be complexed with AL in PAAM networks. The adhesive strength of the hydrogel to the porcine skin was 24.5 kPa with improved proliferation, attachment, and functional expression in human skin fibroblasts. In addition, the hydrogel exhibited rapid blood coagulation within 360 s when treated with porcine whole blood, owing to the PDA catechol groups, although in vivo evaluations were not performed. This is an indication of these hydrogels being promising candidates for skin tissue engineering applications.

Gasek et al. prepared in situ hydrogel TAs composed of DA-conjugated AL methacrylate and DA-conjugated GE methacrylate as pleural and tracheal sealants (Gasek et al., 2021) because both compounds are easily crosslinked owing to the preformed hydrogel patches of the AL-based sealant and in situ hydrogel formation of the GE-based sealant using the photoinitiator Eosin Y and the oxidant triethanolamine. The hydrogels exhibited no air leaks after application to experimentally induced injuries in ex vivo rat lung and tracheal models and in ex vivo pig lungs, allowing full inflation and ventilation of the lungs. In addition, sustained repair of pleural injury in the rat model was observed for up to 1 month, and tracheal injury in the rat model was observed for up to 2 weeks, suggesting further preclinical and clinical applications. This is an indication of the potential of these hydrogels for pleural and tracheal sealants using a pre-formed hydrogel patch.

Zou et al. prepared multi-crosslinked hydrogel TAs composed of DA- and DO-grafted CS methacrylate, aldehyde (ALD)- and boronophenyl (BP)-grafted AL, and TA for hemostasis (Zou et al., 2022). Because DA and DO as the catechol groups in the DA/DO-grafted CS hydrogels can enhance the cohesion in the wet environment, a dynamic covalent bond network between ALD groups and BP groups in the ALD/BP-grafted AL can be produced, and TA can form abundant hydrogen bonds in the hydrogels. The hydrogel exhibited a high adhesion strength of 162.6 kPa on pig skin, which was 12.3-fold that of commercial fibrin glue, owing to the multi-crosslinked networks. Additionally, the hydrogel revealed superior hemostatic ability in rabbit liver injury model with blood loss of 0.32 g, only 54.2 % of that in fibrin glue. This is an indication of these hydrogels being promising candidates for first-aid hemostasis and infected wound healing.

6.2.3.2. Wound dressing. Bai et al. prepared skin tissue-adhesive hydrogel TAs composed of collagen (CO), DO-grafted OAL, and PAAM for cutaneous wound healing (Bai et al., 2018) because CO promotes tissue regeneration, DO-grafted OAL improves the adhesion and cohesion of materials under wet conditions, and crosslinked PAAM enhances the mechanical properties with flexibility. The hydrogel exhibited an adhesion strength of 15 kPa on the porcine skin with good mechanical properties because of the easy reaction of the oxidized DO groups with the amino and mercapto groups on the skin. In addition, the hydrogel accelerated the wound-healing process in full-thickness skin defects in rats. Therefore, these hydrogels have potential applications in cutaneous wound dressings.

Liang et al. prepared injectable self-healing hydrogel TAs with temperature-responsive adhesion composed of protocatechualdehyde (PA), Fe^{3+} , GE, and AL for wound dressing (Liang, Xu, Li, Zhangji, & Guo, 2022) because the carboxyl groups of AL and amino groups of GE

endow the adhesives with cohesion by the ionic interactions between them, PA/ Fe^{3+} enhances the cohesion of the adhesives by the interaction between quinone and aldehyde groups in the PA and amino groups of GE through Schiff base or Michael addition reactions, and GE forms a helical structure through hydrogen bonds at 25 °C while changing random coils at body temperature (Liang et al., 2022). The hydrogels exhibited the rapid mechanical self-healing ability at 37 °C with the injectability due to the dynamic coordination between carboxyl/catechol groups and Fe^{3+} , Schiff base reaction between aldehyde/quinone groups and amino groups of GE, and hydrogen bonds between GE and AL with the temperature-dependent phase transition. The adhesive strength of the hydrogels on porcine skin through a lap shear test was 11–40 kPa with a temperature dependence according to each composition. In addition, the blood loss of the hydrogel in the mouse liver significantly decreased with 110 mg compared to that without treatment with 300 mg. Furthermore, the incisions treated with the hydrogel showed better closure without scarring than those treated with sutures and biomedical glue when wound closure was evaluated using a full-thickness rat skin model. This is an indication of these hydrogels being promising candidates for post-wound-closure and wound dressing due to their property of being reversible adhesive hydrogels.

6.2.3.3. Bone and cartilage regeneration. Hasani-Sadrabadi et al. prepared cell-laden hydrogel TAs composed of DO-AL, methacrylated AL (MAAL), RGD-grafted AL, and hydroxyapatite (HAP) microparticles (MPs) for craniofacial bone tissue regeneration (Hasani-Sadrabadi et al., 2020) because DO-AL shows strong adhesion to tissues in the presence of blood or saliva, MAAL can be cross-linked by visible light irradiation, HAPMPs induce osteogenic differentiation of encapsulated gingival mesenchymal stem cells (GMSCs), and RGD as a co-mimicking short peptide provides strong cell adhesion through DO. These hydrogels exhibited biodegradability, biocompatibility, and osteoconductivity after subcutaneous implantation in mice. In addition, the hydrogel promoted complete bone regeneration around dental implants with peri-implant bone loss in a rat peri-implantitis model. Therefore, these hydrogels are promising candidates for craniofacial tissue engineering applications given the loaded stem cells and hydroxyapatites present in the TAs.

Öztürk et al. prepared a tyrosinase-crosslinked hydrogel TAs composed of sulfated and tyramine-modified AL for cartilage repair (Ozturk et al., 2020) because the sulfated group mimics the high glycosaminoglycan content of cartilage, and the tyramine group allows in situ enzymatic crosslinking with tyrosinase under physiological conditions (An et al., 2018). The hydrogels exhibited viability of loaded bovine chondrocytes and showed a strong increase in the expression of chondrogenic genes such as aggrecan, CO 2, and Sox 9. In addition, the human chondrocyte-loaded hydrogels showed potent deposition of the cartilage matrix components CO 2 with in vivo stability upon subcutaneous implantation into mice for 4 weeks due to strong adhesion to cartilage and chondrogenic re-differentiation. This indicates the potential of these hydrogels in cartilage tissue engineering applications.

6.2.3.4. Drug delivery. Kim et al. prepared microRNA-141 (miRNA-141)/polyallylamine (PAL) complex-loaded hydrogel TAs composed of miRNA-141/PAL complexes and OAL for the locoregional treatment of hepatocellular carcinoma (HCC) with long-term therapeutic effectiveness (Kim et al., 2018a) because the miRNA-14/PAL complexes can generate TA hydrogels after mixing with OAL through the Schiff base reaction. The complex-loaded TAs led to the efficient delivery of miRNA-141 to cultured cells and solid tumors in mice while maintaining their gene expression for up to 30 d. In addition, they dramatically retarded tumor growth compared with the negative control upon intratumoral injection into the mouse skin, suggesting potential locoregional treatment of HCC in a long-term manner using complex-loaded TAs. This is an indication of these hydrogels being promising candidates for anti-

cancer gene delivery systems using TAs.

Koh et al. prepared triamcinolone acetonide (TRA)-loaded tunable tough hydrogel TAs composed of AL/PAAM as the tough hydrogel dissipative matrix, CS as the adhesive surface, and TRA-loaded laponite NPs of PLGA MPs for the local release of drugs to tissues in an extended manner (Koh et al., 2023). The Ca^{2+} -crosslinked/covalently crosslinked PAAM allows for strong adherence to the target tissue with controlled drug delivery (Li et al., 2017). Additionally, the laponite NPs or PLGA MPs control the sustained release of TRA owing to their ionic and hydrogen bonds with the TRA (Li et al., 2018). This is an indication of these hydrogels being promising candidates for controlled drug delivery systems using tunable tough TAs.

6.2.3.5. Bioelectronics. Kim et al. recently prepared conductive and TA hydrogels composed of DO-conjugated AL and poly (3,4- ethylene dioxythiophene) (PEDOT)/poly (styrene sulfonate) (PSS) for on-tissue writable bioelectronics (Kim et al., 2023b) because Ca^{2+} ion-crosslinked DO-conjugated AL allows TA properties with mussel-inspired CA moieties, and PEDOT/PSS has been used as a wet-conducting polymer with high conductivity (Feig et al., 2021). Granular hydrogels fabricated through an electrohydrodynamic spraying method exhibited an adhesive strength of approximately 6 kPa on porcine skin tissue under tensile stress, with shear-thinning and injectable properties. In addition, the hydrogels showed a conductivity of 0.4 Sm^{-1} with an effective function as an electrode on the skin tissue surface, an indication of potential application for bioelectronics, although in vivo experiments were not performed. Similarly, Perkucin et al. prepared bioinspired conductive TA hydrogels composed of DO-conjugated AL, NaIO_4 as an oxidizing agent, and graphene as a conductive carbon-based nanofiller for electrical stimulation-based therapies in neural regenerative medicine (Perkucin, Lau, Morshead, & Naguib, 2022) because DO-conjugated AL can be crosslinked in the presence of NaIO_4 and graphene is a conductive nanofiller. The resulting hydrogels exhibited gelation times ranging from 8 to 35 min according to the concentrations of graphene and NaIO_4 . In addition, 1 wt.-% graphene-loaded hydrogel showed conductivity values on the order of $2.3 \times 10^{-4} \text{ Scm}^{-1}$ with an adhesion energy of 1.793 Jm^{-2} to bovine cartilage without cytotoxicity to brain-derived neural precursor cells. This is an indication of these hydrogels being promising candidates for soft and flexible electronics to connect humans and machines by TAs.

6.2.3.6. Tendon healing. Freedman et al. prepared tough hydrogel TAs composed of Ca^{2+} -ion-crosslinked AL to dissipate energy, highly elastic covalently crosslinked PAAM, and CS to create an adhesive surface for

enhanced tendon healing (Freedman et al., 2022) because a dual interpenetrating hydrogel network can be formed between the ionically crosslinked AL and covalently crosslinked PAAM, and CS, as a TA site, can be unilaterally coupled to the AL/PAAM hydrogel. The resulting hydrogel exhibited strong adhesion greater than 1000 J/m^2 to the porcine tendon owing to the dissipative tough matrix on one side and a CS adhesive surface on the opposite surfaces. In addition, the hydrogel boosted healing and reduced scar formation in a rat model of Achilles tendon rupture with the controlled release of TRA. This is an indication of these hydrogels being promising candidates for tendon healing due to presence of a Janus surface and sustained-drug-release system.

6.2.3.7. Colon-targeting. Liu et al. prepared a colon-targeted TA hydrogel composed of Ca^{2+} -loaded thiolated hyaluronic acid (THA) microspheres crosslinked by silver ions as the hydrogel core using gas-shearing technology and a Ca^{2+} -AL hydrogel formed by ionic cross-linking between AL and diffused Ca^{2+} from the Ca^{2+} -loaded THA to regulate gut immunity and flora as shown in (Fig. 10) (Liu et al., 2021) because THA showed anti-inflammatory properties (Siddiqi, Husen, & Rao, 2018), and Ca^{2+} -AL microspheres were used for colon-targeted delivery (Agüero, Zaldivar-Silva, Peña, & Dias, 2017). The hydrogel microspheres exhibited aggregation in the inflamed colon mucosa of mice and resulted in prolonged local drug dwell time due to colon targeting by AL and the mucoadhesive property of THA. In addition, THA microspheres suppressed the secretion of proinflammatory cytokines and augmented probiotic abundance by restraining the detrimental bacterial community. Furthermore, hydrogel microspheres remarkably alleviated colitis in mouse models. This is an indication of their potential as clinical candidates for inflammatory bowel disease because they are colon-targeted adhesive hydrogel microspheres.

6.2.3.8. Cornea regeneration. Farasatkia et al. prepared a double-layer micro-patterned TA film composed of silk nanofibrils-incorporated methacrylated GE as the anisotropic layer and ascorbic acid (AA)-loaded AL as the adhesive layer for corneal regeneration (Farasatkia & Kharaziha, 2021) because the silk nanofibrils have good mechanical properties with excellent biocompatibility and crosslinked methacrylated GE by the UV-irradiation can provide similarly a natural extracellular matrix environment for the biological properties of the regeneration, and the crosslinked-AL by Ca^{2+} can provide strong adhesion on the endothelium layer of the cornea with an excellent antioxidant of released AA from the AA-loaded AL (Luo, Lai, Chou, Hsueh, & Ma, 2018). The double-layer TA film exhibited the adhesion and orientation of corneal stromal cells with mechanical robustness and 90

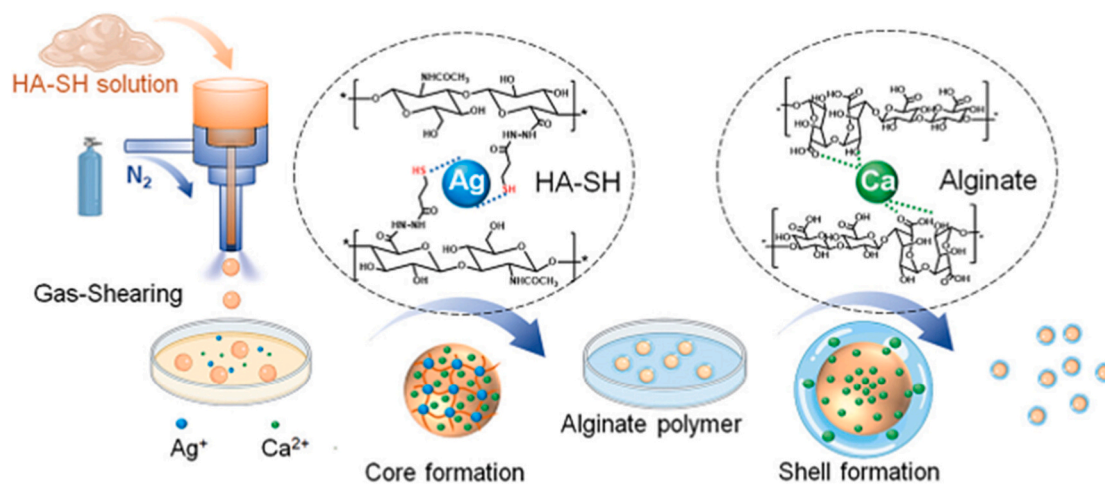


Fig. 10. Method of fabrication of THA/Ag microspheres as the Core and Ca^{2+} -AL hydrogel as the shell. [Adapted from Liu et al., 2021 with permission from John Wiley and Sons.]

% light transmission, although the tensile strength of the film was approximately 3 MPa owing to the micropattern size. Additionally, the adhesion strength of crosslinked AL on sheep skin in wet conditions was approximately 47 ± 4 kPa, which is higher than commercial corneal glues such as Evicel, Quixil, and Beriplast. Furthermore, AA significantly promoted corneal stromal cell attachment, proliferation, and alignment compared to the AA-free film, although this was not observed in vivo. This is an indication of these hydrogel being promising candidates for stroma tissue engineering applications because they have the property of being a micro-patterned double-layer film.

A list of applications using AL-based TAs is shown in Table 2.

6.2.4. Advantages and disadvantages

One major application of AL has been in wound dressings (Aderibigbe & Buyana, 2018) because a dried AL wound dressing absorbs wound exudate rapidly and provides a moist environment to the wound site to promote wound healing. AL oxidized by sodium periodate can be converted into hydrolytically labile bonds, although AL is non-degradable in the body and creates aldehydes to be used with a cross-linker presenting amines for the formation of TA (Nam & Mooney, 2021). However, the content of the G and M blocks depends on the natural source, which affects the physicochemical properties of AL. In addition, ionically cross-linked AL can be easily dissolved in water owing to the loss of divalent ions such as Ca^{2+} and Mg^{2+} .

6.3. Dextran (DE)

6.3.1. Characteristics

DE mainly consists of α -1,6-glycosides with small α (1,3) branches and high water-binding ability due to the dense hydroxyl groups in the backbone (Shaz & Hillyer, 2013). It has been used in medicine as a volume expander to treat hypovolemia and as an inhibitor of thrombocyte aggregation and coagulation factors to reduce blood viscosity, although it does not contain tissue-reactive functional groups in its original form (Nam & Mooney, 2021).

6.3.2. Mechanism of adhesion based on functional groups in adhesives

Pang et al. prepared mechanically strengthened hydrogel TAs comprising carboxymethyl CS (CMCS), DE dialdehyde (DED), and chitin nanowhiskers (CNW) for rapid hemostasis (Pang et al., 2020). This was performed because the incorporation of CNW into the complexed hydrogel between the amino groups of CMCS and the aldehyde groups of DED through the Schiff base reaction affecting the cross-linking of the hydrogel. Additionally, the wound was immediately covered by the hydrogel due to gel formation.

Liu et al. prepared in situ wet-adhesive sponge-type TAs for rapid hemostasis by simple lyophilization of oxidized DE without using any crosslinkers (Liu et al., 2019). This was performed DE has high water-binding ability, and sponges can rapidly absorb blood to control bleeding, indicating that hemostasis occurred through imine bond formation between the aldehyde groups of DE and the amine groups of the tissue.

Hyon et al. prepared self-degradable hydrogel TAs composed of aldehyde DE (ADE) and succinyl ϵ -poly-L-lysine (SPLL) for use as hemostatic materials (Hyon et al., 2022). This type of hydrogel was produced because gelation and adhesion of ADE/SPLL were achieved through Schiff base bond formation between the aldehyde groups of ADE and the amino groups of SPLL.

Chen et al. prepared hydrogel TAs composed of ODE, CS, and DO to enhance adhesiveness (Chen et al., 2023b) because the cohesion and adhesion of the ODE/CS hydrogel were improved by in situ mixing with DO. Additionally, multi-crosslinked hydrogels were further prepared by adding sodium periodate or ferric trichloride (FT) as crosslinking agents. In addition, the lap shear adhesion strength of ODE/CS/DO/FT in porcine skin was 43-fold higher than that of fibrin glue owing to the coordination of Fe^{3+} and DO and the non-covalent and covalent bonds of DO.

Chen et al. prepared triple-networks hydrogel TAs composed of carboxymethyl CS (CMCS), ODE, and γ -polyglutamic acid (γ -PGA) for hemostasis of incompressible bleeding under wet wound conditions (Chen et al., 2023c). These hydrogels were created because the amino

Table 2

A list of applications using AL-based TAs.

Category	Main components	In vivo model	Target tissue	Results	Reference
Hemostatic agents	Polydopamine, alginate, polyacrylamide	Non-treatment	Non-treatment	High adhesive strength due to the good hemostatic properties of polydopamine	(Suneetha et al., 2019)
	Alginate methacrylate, gelatin, methacryloyl, dopamine	Rat	Lung	Good hemostatic properties due to the adherence properties of dopamine	(Gasek et al., 2021)
	Carboxymethyl chitosan, alginate, tannic acid, dopamine	Rat	Skin	Strong hemostatic performance due to the multi-crosslinking	(Zou et al., 2022)
Wound dressing	Dopamine, collagen, polyacrylamide, alginate	Rat	Skin	Accelerated wound healing due to the high toughness and good adhesion	(Bai et al., 2018)
	Gelatin, protocatechol aldehyde, ferric ion, alginate	Rat	Skin	Promotion of wound healing due to the thermos-responsive reversible adhesion	(Liang et al., 2022)
Bone and cartilage regeneration	Mesenchymal stem cells, hydroxyapatite, dopamine, RGD alginate	Mouse	Bone	Promotion of bone regeneration due to the loaded stem cells and hydroxyapatite	(Hasani-Sadrabadi et al., 2020)
	Tyrosinase, tyramine, alginate, chondrocytes	Mouse	Cartilage	Fast cartilage repair due to the strong adhesion and chondrogenic re-differentiation	(An et al., 2018)
Drug delivery	Poly(allyl amine), microRNA-141, alginate	Mouse	Skin	Dramatic retardation of tumor due to the loaded microRNA-141	(Koh et al., 2023)
	Poly(acryl amide), triamcinolone acetonide, alginate, laponite, chitosan, poly(L-lactic-co-glycolic)	Non-treatment	Non-treatment	Anti-inflammatory functions in vitro due to the stimuli-responsive drug delivery	(Freedman et al., 2022)
Bioelectronics	Dopamine, Ca^{2+} , poly(3,4-ethylene dioxythiophene), poly(styrene sulfonate), alginate	Non-treatment	Non-treatment	Similar conductivity to muscle tissue due to the conductive polymers	(Feig et al., 2021)
	Dopamine, graphene, alginate	Non-treatment	Non-treatment	Good electrical properties due to the loaded graphene	(Freedman et al., 2022)
Tendon healing	Poly(acryl amide), chitosan, Ca^{2+} , alginate, triamcinolone acetonide	Rat	Tendon	Enhanced tendon healing due to the loaded drug	(Liu et al., 2021)
Colon-targeting	Hyaluronic acid, Ca^{2+} , Ag^+ , alginate	Mouse	Colon	Remarkable alleviation of colitis due to the mucoadhesive hyaluronic acid	(Siddiqi et al., 2018)
Cornea regeneration	Silk, gelatin, ascorbic acid	Non-treatment	Non-treatment	Significant promotion of corneal stroma cells behaviors due to the loaded drug	(Luo et al., 2018)

groups of CMCS can react with the carboxyl groups of γ -PGA and the aldehyde groups of ODE through amide and Schiff base bonds, respectively.

6.3.3. Applications

6.3.3.1. Hemostasis. Chen et al. prepared triple-network hydrogel TAs composed of methacrylate GE (MGE), ODE, and borax for effective non-compressible visceral hemostasis (Chen et al., 2021) because MGE can be cross-linked by the UV crosslinking agent Igracure 2959, the aldehyde groups of ODE are crosslinked with amino groups on the tissue surface through Schiff base bonds and borax forms a boric acid ester bond between borax and ODE. The hydrogel exhibited excellent hemostatic ability and prevented bleeding of the puncture lesion within 30 s, with accelerated wound healing and anti-microbial properties in a rat liver model.

Sun et al. prepared absorbable sponge-type hydrogel TAs composed of ODE, carboxymethyl CS (CACS), and PDO-NPs to achieve hemostasis and effective infection resistance as shown in (Fig. 11) (Sun et al., 2022) because ODE/CACS acts as a scaffold for the wound dressing platform and blood absorption activity, and the PDO-NPs act as a photothermal agent for anti-microbial therapy and as an active site for thrombin immobilization. The sponge exhibited a significantly lower amount of blood than commercially available hemostatic dressings because of the thrombin adsorbed on the lyophilized ODE/CACS/PDO-NP sponge. In addition, the sponge exhibited significantly accelerated wound healing owing to its rapid hemostatic activity and effective infection resistance. This is an indication of these hydrogel being promising candidates for hemostasis and wound healing due to their multifunctional properties.

Zhu et al. prepared in situ injectable self-healing hydrogel TAs composed of choline phosphoryl (CP)-grafted CS (CPCS) and ODE for enhanced hemostasis, as shown in (Fig. 12) (Zhu et al., 2023b) because the CP in CPCS has been reported to be a biomembrane-adhesive molecule through ionic interactions between the CP and phosphatidylcholine groups (Yu et al., 2012), and ODE can be crosslinked through an aldehyde-amine Schiff base reaction. The hydrogel exhibited enhanced blood clotting and erythrocyte adhesion/aggregation abilities owing to the incorporation of CP in the CS compared to those of the CS/ODE hydrogel, although the gelation time, tissue adhesiveness, and hemostatic ability were dependent on the CD and aldehyde contents in the CPCS and ODE, respectively. In addition, the hydrogel showed higher hemostatic ability than CS/ODE and a commercial fibrin sealant in rat tail amputation and liver/spleen injury models. This is an indication of these hydrogel being promising candidates for hemorrhage control due

to the choline phosphoryl groups in the TAs.

6.3.3.2. Wound dressing. Yin et al. prepared multifunctional hydrogel TAs composed of ODE and rosmarinic acid (RA)-grafted aminated GE for wound dressing (Yin et al., 2023) because the catechol structure of RA can enhance tissue adhesiveness due to the similarity of DO and the RA has several biological activities such as anti-inflammatory, antiviral, antibacterial, antioxidant, and anticancer (Ghasemzadeh Rahbardar & Hosseinzadeh, 2020), and the ODE forms hydrogel with RA-grafted aminated GE through Schiff base reaction. The hydrogel exhibited a fast gelation time of 61.6 ± 2.8 s strong adhesive strength of 27.30 ± 2.02 kPa and enhanced mechanical property of 1.31×10^4 Pa. In addition, the amount of collagen deposition and CD31 on wounds for the hydrogel on day 14 was 4.3-fold and 2.3-fold that of the control group in a rat model of full-thickness skin-defect due to the grafted RA in the hydrogel. This is an indication of these hydrogel being promising candidates for wound dressing due to their multifunctional properties.

Du et al. prepared injectable hydrogel TAs composed of dodecyl aldehyde-grafted CS (DACS) and ODE for wound healing (Du et al., 2019) because in situ gelation occurs by the reaction of the amino groups of DACS and the aldehyde groups of ODE through a Schiff-based bond and hydrophobic interactions. The gelation time of the hydrogel decreased significantly from 343 to 90 s and the adhesive strength on porcine skin increased from 3.8 to 8.9 kPa as the ODE concentration increased from 1 to 4 wt.-%. In addition, the wounds in a full-thickness infected skin defect rat model were almost completely healed with the hydrogel compared to the control group on day 15. Therefore, these hydrogels are promising candidates for hemorrhagic and infected wound healing due to their multifunctional properties.

6.3.3.3. Lung injury. Balakrishnan et al. prepared an in situ-forming TA hydrogel composed of dialdehyde DE (DDE) and CS to seal lung injuries (Balakrishnan, Payanam, Laurent, Wassef, & Jayakrishnan, 2021) because in situ gelation occurred within 4 s owing to the reaction of the aldehyde groups in DDE with the amino groups in CS through Schiff's reaction. The hydrogel completely sealed the sheep lung incision site even during inflation, with an airway pressure of 30 cm of water without air leakage. In addition, the hydrogel effectively sealed aortic incisions in a pig model without aneurysms. This is an indication of these hydrogels being promising candidates as a sealant for the prevention of air and blood leaks following lung and vascular surgery.

6.3.3.4. Bone regeneration. Wang et al. prepared injectable complex hydrogel TAs composed of bisphosphonate (BP)- and adipic dihydrazide

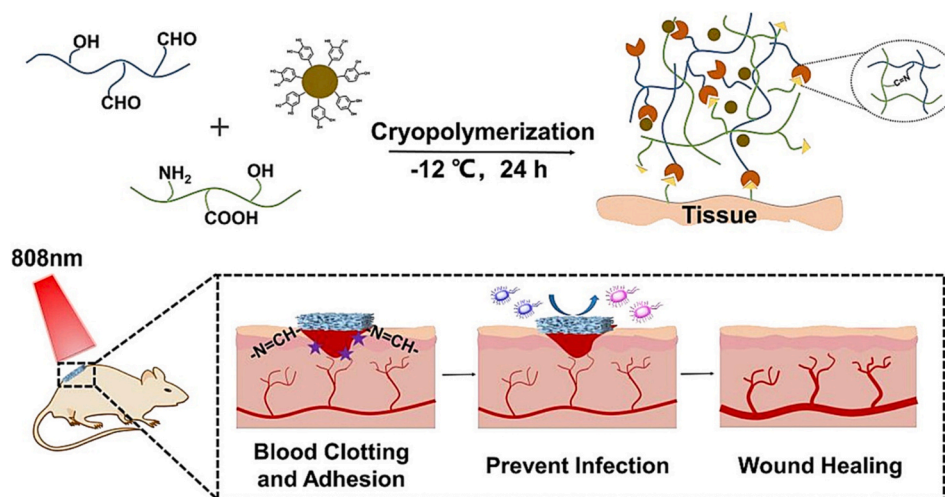


Fig. 11. Schematic explanation of the preparation of sponges and their application as antibacterial and wound dressing materials. [Adapted from Sun et al. (2022) with permission from Elsevier.]

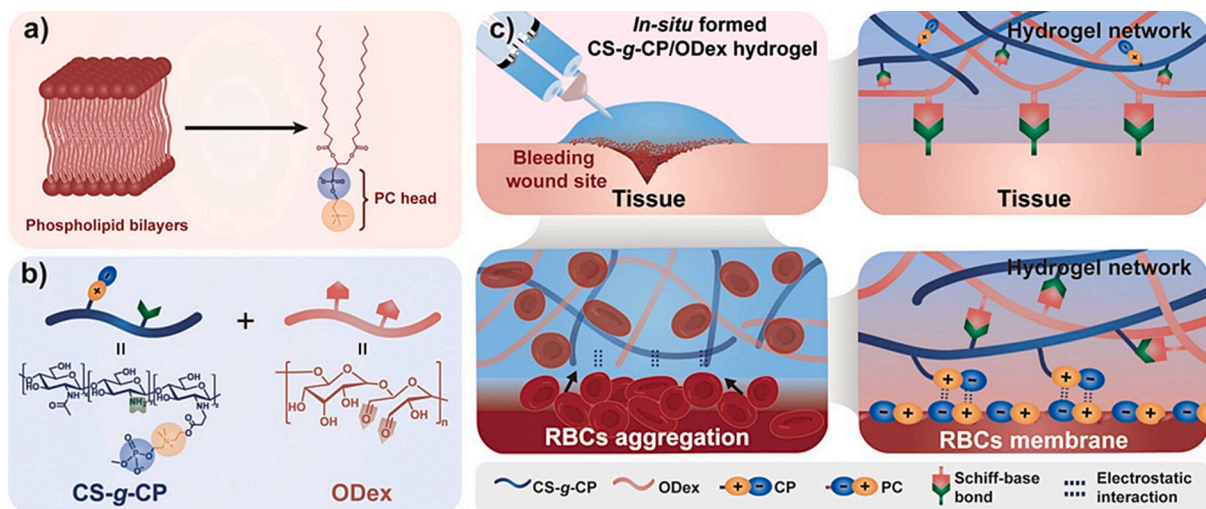


Fig. 12. (a) Schematic illustration of the phospholipid bilayer. (b) The structure of zwitterionic chitosan derivatives CS-g-CP and ODex. (c) Schematic illustration of the hemostatic mechanism of the CS-g-CP/ODex hydrogels.

[Adapted with permission from [Zhu et al. \(2023b\)](#). Copyright (2023) American Chemical Society.]

(AD)-PLGA, aldehyde- and CA-conjugated DE, and HAT NPs for bone regeneration ([Wang et al., 2021](#)) because non-covalent chelation between BP and HAT induced the formation of physical hydrogels and intermolecular Schiff base reactions between the hydrazide groups in BP-AD-PLGA and the aldehyde groups in the dually cross-linked hydrogels. The hydrogel exhibited good tissue adhesion owing to multiple adhesion ligands, such as CA, BP, and aldehyde groups. In addition, the introduction of BP and HAP NPs promoted the proliferation, migration, and osteogenesis of MC3T3-E1 cells, thereby facilitating the angiogenic properties of endothelial cells. Furthermore, the hydrogel exhibited significantly more newly formed bone tissue in rat cranial defects from the 4th week than in the untreated group. This is an indication of these hydrogel being promising candidates for bone regeneration applications due to the osteogenic injectable TA.

6.3.3.5. Periodontal disease. Lin et al. prepared injectable melatonin (MT)-loaded hydrogel TAs composed of CACS and ODE for the treatment

of periodontal disease ([Lin, Lv, Wang, & Liu, 2023](#)) because in situ gelation occurs by the reaction of amino groups in CACS and aldehyde groups in ODE through the Schiff base reaction, and MT possesses several biological activities, such as tissue repair promotion, immunoregulation, antitumor effects, and antioxidant activity ([Maleki et al., 2021](#)). The hydrogel exhibited high tissue adhesion to the wet surface of the pigskin and a motional state with injectability. In addition, the hydrogel promoted L92 cell migration due to the release of MT from the MT-loaded hydrogel, although this was not observed in vivo. This is an indication of these hydrogel being promising candidates for treatment of periodontal disease due to the presence of loaded melatonin in the TAs.

6.3.3.6. Infarcted myocardium. Wu et al. prepared mesenchymal stem cells (MSCs)-loaded wet adhesive hydrogel composed of hydrazided HA (HHA), resveratrol (RE)-complexed 3-hydroxypropyl cyclodextrin (RE-C-HP- β -CL) and ODE for infarcted myocardium as shown in ([Fig. 13](#)) ([Wu et al., 2023b](#)) because the HHA can prolong the in vivo retention

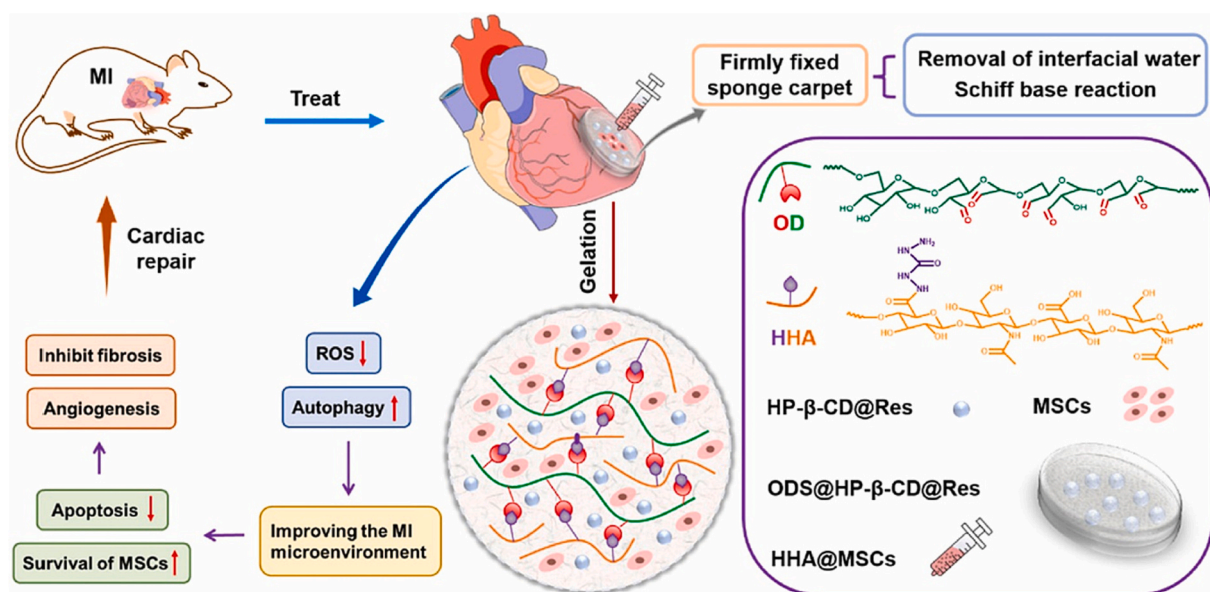


Fig. 13. Schematic illustration of the design of adhesive hydrogel system for the treatment of myocardial infarction.

[Adapted from [Wu et al. \(2023b\)](#) with permission from Elsevier.]

time of loaded drug and cells after in situ gelation through click reaction, the RE-C-HP- β -CD can improve cardiac microenvironment, reduce cardiomyocyte apoptosis, and the Schiff base reaction between the aldehyde groups on ODE and amino groups on the myocardium tissue. Interestingly, the addition of encapsulated MSCs to the outer ODE surface sponge consumed the remaining aldehydes to form a non-sticky top surface, avoiding adhesion to other tissues. The hydrogel composed of MSC-loaded HHA/RE-C-HP-CD/ODE exhibited the highest therapeutic efficiencies in myocardial infarction of rats. This is an indication of these hydrogel being promising candidates for the restoration of infarcted myocardium due to the facilitating angiogenesis and reduction of cardiac fibrosis.

6.3.3.7. Bioelectronics. Tondera et al. prepared conductive and stretchable hydrogel TAs composed of nano clay Laponite (NLA), poly(ethylene-3,4-diethoxy thiophene) (PEDOT), and PAAM for tissue-mimetic neuro stimulating electrodes (Tondera et al., 2019) because the NAL dramatically increases the conductivity of in-scaffold polymerized PEDOT and the crosslinked PAAM network obtained by UV light irradiation enhances the mechanical strength for use in potential bioelectronic devices. The hydrogel exhibited an electrical conductivity of 26 Sm⁻¹, stretchability of 800 %, and tissue-like elastic modulus of 15 kPa. The NLA dramatically increased the conductivity of the in-scaffold PEDOT without other dopants. In addition, the scaffold coated with adhesive peptide and dextran sulfate enhanced the neuronal differentiation of human-induced pluripotent stem cells on the surface of the conductive hydrogels, although this was not examined in vivo. This is an indication of these hydrogel being promising candidates for tissue-mimetic neuro stimulating electrodes due to the presence of conductive and stretchable TA.

A list of applications using DE-based TAs is shown in Table 3.

6.3.4. Advantages and disadvantages

DE has been used in TA, mostly in an oxidized form with aldehyde groups from the backbone through oxidation using sodium periodate. The aldehyde groups in ODE undergo Schiff base reactions with the amine groups of the crosslinkers, leading to in situ gelation. A simple lyophilized DE sponge can be used as a hemostatic TA through imine bond formation between the aldehyde groups in ODE and the amine groups in the tissue. In contrast, the degradation rate of ODE TA was relatively fast (approximately 3 d) owing to the hydrolysis of imine

bonds. In addition, a large amount of TA was required to obtain adequate sealing and adhesion properties (Bhatia et al., 2007).

6.4. Hyaluronic acid (HA)

6.4.1. Characteristics

HA, a non-sulfated anionic polysaccharide, is a linear polymer consisting of alternating β -(1,3)-linked *N*-acetyl-D-glucosamine and β -(1,4)-linked D-glucuronic acid (Dicker et al., 2014). HA regulates the viscoelasticity of joint synovial and eye vitreous fluids and maintains tissue hydration owing to its high water-binding capacity (Necas, Bartosikova, Brauner, & Kolar, 2008). HA has been used in a wide range of clinical applications, such as viscosupplementation for arthritis, surgical aid in ocular surgery, and wound dressing (Goa & Benfield, 1994).

6.4.2. Mechanism of adhesion based on functional groups in adhesives

Kim et al. prepared enzyme-mediated TA hydrogels composed of tyramine (TA)-conjugated HA, GE, and tyrosinase (TYR) for meniscus repair (Kim et al., 2018b). This was performed because TYR forms covalent bonds with amines, thiols, and imidazoles under mild conditions through the oxidation of phenolic groups (Ramsden & Riley, 2014). Additionally, TYR-oxidized TA generates quinone groups, and these quinones form covalent bonds with other phenolic moieties through non-enzymatic reactions, and GE forms covalent bonds with the quinones through Michael-type addition (Tan, Chu, Payne, & Marra, 2009). The same group reported another enzyme-mediated TA hydrogel using a novel tyrosinase derived from *Streptomyces avermitilis* (SA-TY) (Kim et al., 2018b, 2018c).

Sani et al. prepared zinc oxide (ZnO)-loaded elastic hydrogel TAs composed of methacrylated HA (MHA), an elastin-like polypeptide (ELP) with photopolymerizable cysteine groups, and ZnO for cartilage repair (Shirzaei Sani et al., 2018). This was performed because hybrid hydrogels can be obtained by the free radical photopolymerization of MHA and crosslinked ELP by the disulfide bonds present in the cysteine groups in the ELP using a photoinitiator.

Bermejo-Velasco et al. prepared aldol-cross-linked hydrogel TAs composed of enolizable aldehyde-HA (EHA) and non-enolizable aldehyde-HA (NEHA) to obtain fast and hydrolytically stable hydrogels for bonding two bone tissues (Bermejo-Velasco et al., 2019). This was performed because the mixing of EHA and NEHA, leading to hydrolytically stable hydrogels owing to stable C—C bond formation, although

Table 3

A list of applications using DE-based TAs.

Category	Main components	In vivo model	Target tissue	Results	Reference
Hemostasis	Gelatin, borax, dextran	Rat	Liver, heart	Effective hemostasis due to the blocking bleeding by the triple-network structure	(Sun et al., 2022)
	Carboxymethyl chitosan, polydopamine, dextran, thrombin	Mouse	Liver	Rapid hemostatic properties due to the loaded thrombin	(Yin et al., 2023)
	Chitosan, choline phosphoryl, dextran	Rat	Liver, spleen	Improved hemostatic ability due to the biomembrane adhesive molecule of choline phosphoryl	(Yu et al., 2012)
Wound dressing	Rosmarinic acid, gelatin, dextran	Rat	Skin	Promotive wound healing due to the anti-inflammatory activity of rosmarinic acid	(Ghasemzadeh Rahbardar & Hosseinzadeh, 2020)
	Chitosan, dodecyl aldehyde, dextran	Rat	Skin	Accelerated wound healing due to the antibacterial properties by chitosan	(Balakrishnan et al., 2021)
Lung injury	Chitosan, dextran	Sheep	Lung	Complete sealing of lung incision site without using any extraneous cross-linking	(Wang et al., 2021)
Bone regeneration	Hydroxyapatite, poly(L-glutamic acid), bisphosphonate, dextran, dopamine	Rat	Cranium	Significantly fast bone tissue regeneration due to the hydroxyapatite and bisphosphonate	(Lin et al., 2023)
Periodontal disease	Melatonin, carboxymethyl chitosan, dextran	Non-treatment	Non-treatment	Promoted L929 cell migration in vitro due to the melatonin	(Maleki et al., 2021)
Infarcted myocardium	Hyaluronic acid, resveratrol, β -hydroxy propyl cyclodextrin, dextran, mesencymal stem cells	Rat	Myocardium	Promoted cardiac repair due to the loaded resveratrol and mesencymal stem cells	(Tondera et al., 2019)
Bioelectronics	Laponite, poly(ethylene-3,4-diethoxy thiophene), adhesive peptide, dextran	Non-treatment	Non-treatment	Highly conductive properties due to the loaded laponite	(Bhatia, Arthur, Chenault, Figuly, & Kodokian, 2007)

hydrogel degradation occurred through a hyaluronidase-mediated enzymatic mechanism.

Zhou et al. prepared composite hydrogel TAs composed of DO-conjugated HA (DHA) and poly(L-lysine) (PLL) for wound closure (Zhou, Kang, Yue, Liu, & Wallace, 2020). This was performed because the DO groups in DHA provide strong single-molecule adhesion to both organic and inorganic surfaces under wet conditions, and the use of PLL as a bridging polymer improves tissue adhesion with an improvement in cellular behavior owing to the penetration of PLL into the native tissue and provided more binding sites for DO-HA. Another group prepared a DO-HA macromer by a Schiff base reaction between DO and dialdehyde-modified HA to achieve fast formation and high TA of DO-HA because this reaction improved the degree of substitution (DS) of the DO groups (Zhou et al., 2020).

Samanta et al. prepared injectable scaffold-type hydrogel TAs composed of hydrazine-cross-linked HA (HA-HA) between aldehyde and carbodihydrazide (CAD) groups in aldehyde-and CAD-grafted HA, and hydrazone crosslinked and gallol (GA) crosslinked HA (HA-GA) between aldehyde and CAD in aldehyde-and-CAD-grafted HA, and aldehyde and GA/CAD-grafted HA for viable immunotherapeutic interventions, as shown in (Fig. 14) (Samanta et al., 2022).

Panday et al. prepared nanocomposite hydrogel TAs composed of DO-HA and PDO NPs to obtain an improved tissue glue (Pandey et al., 2022). This was performed because PDO NPs can enhance the tissue adhesion of DO-HA alone, although the adhesiveness of the hydrogel is dependent on the size and concentration of PDO NPs.

Zhang et al. prepared aminion-derived conditioned medium (AMCM)-loaded in situ gelation hydrogel TAs composed of MA- and *N*-(2-aminoethyl)-4-[4-(hydroxymethyl)-2-methoxy-5-nitrophenoxy]-butanamide (NP)-grafted HA for diabetic wound repair (Zhang et al., 2022). This hydrogel photopolymerized in situ within 3 s through free-radical crosslinking, and formed *o*-nitroso benzaldehyde groups by photo-irradiation covalently bonded with the amine groups of the tissue surface.

Qiu et al. prepared lubricating TA hydrogels composed of OHA and *N*-(2-hydroxypropyl)-3-tri-methylammonium CS polymethacrylate

(HTCSPMA) for articular regeneration by Schiff base reaction between aldehyde groups in OHA and amino groups in HTCSPMA, and covalently crosslinking of the HTCSPMA using photo-irradiation (Qiu et al., 2023). The hydrogels showed appropriate rheological property for self-healing capability. Also, the hydrogels exhibited stable TA property due to the formation of dynamic covalent bonds with the rabbit cartilage surface. Furthermore, the hydrogels exhibited a robust regeneration of articular cartilage of rabbit with the biocompatible and biodegradable properties.

Peng et al. prepared tough and biomimetic TA hydrogels composed of crosslinked HA and poly(*N*-hydroxyethyl acrylamide) (PHEA) for wound healing (Peng et al., 2023) by chemically crosslinked methacrylated HA and HEA using double networks including sol-gel and UV irradiation methods. The multiple hydrogen bonding of the hydrogels provides significant increase in mechanical properties and high adhesiveness on biological tissues. The hydrogels exhibited a low hemolysis ratio of 5 % and high cell viability of 99 %. Also, the wound healing rate of the hydrogels in rat skin defect model was approximately 98 % on day 15, higher than that of the control group, due to promotion of epithelialization, collagen deposition, and angiogenesis by the hydrogel although it is dependent on the ratio of HA/PHEA. This is an indication of these hydrogel being candidates for wound healings through the tough and biomimetic properties.

Zhu et al. prepared pH- and light-responsive nanocomposite TA hydrogels composed of DA-modified GE, Cu-loaded PDA nanoparticles (CuPDA NPs), phenyl borated HA (PBHA), and metformin (MF) for diabetic infected wound healing (Zhu et al., 2023a). The Cu^{2+} accelerates wound healing with antibacterial property (Marelli et al., 2015), PDA has been used as photothermal therapy (Guo et al., 2022b), and MF can decrease inflammation and oxidative stress (Buldak et al., 2014). The hydrogels effectively inhibited the inflammation by elimination of POS with antibacterial property due to the slow release of MF and Cu^{2+} , and the pH- and light-sensitive properties of the hydrogels. Also, the hydrogels significantly promoted wound healing of diabetic rat due to the antibacterial property, inhibition of inflammation, increase of angiogenesis, and acceleration of ECM by the hydrogels. This is an indication of these hydrogel being candidates for diabetic wound

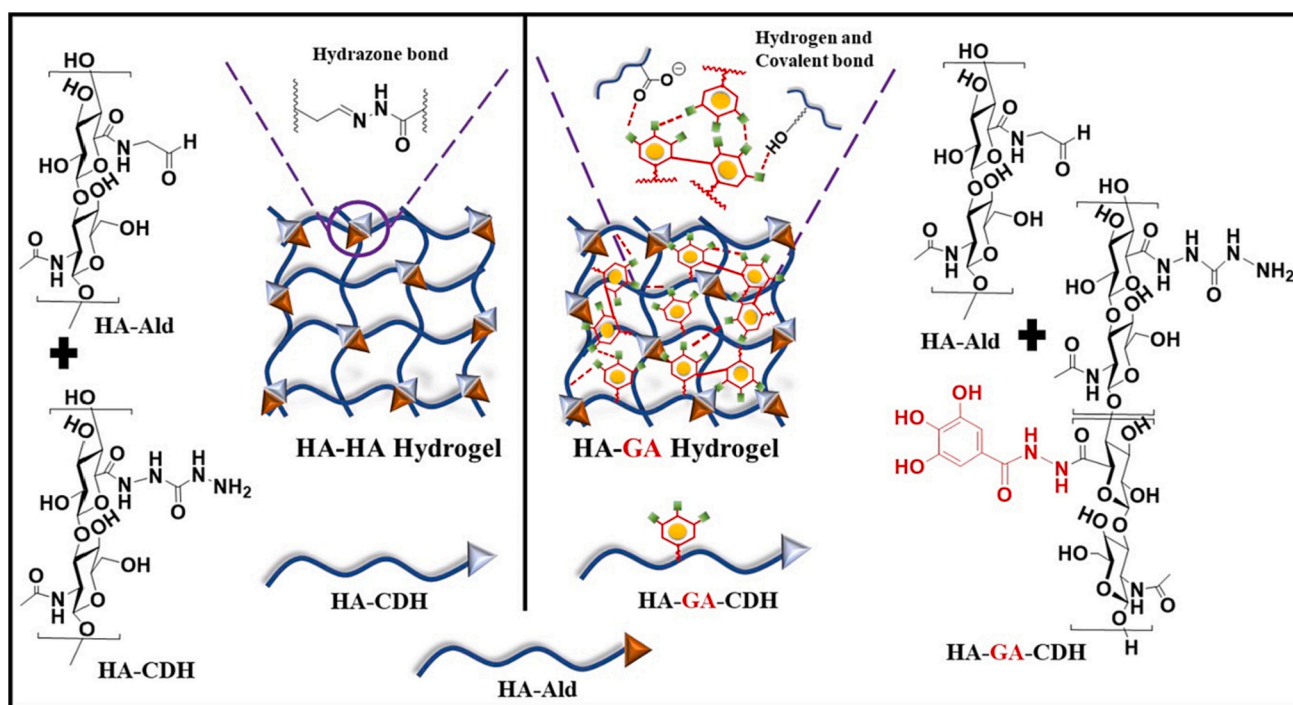


Fig. 14. Schematic representation of the formation of hydrazone crosslinked HA-HA and hydrazone and gallol crosslinked interpenetrating HA-GA hydrogel. [Adapted from Samanta et al., 2022 with permission from Elsevier.]

healing due to pH- and light-sensitive properties of TAs.

6.4.3. Applications

6.4.3.1. Hemostasis. Li et al. prepared single-component HA hydrogel TAs based on phenyl boronic acid (PA)-diol ester linkages for hemostasis (Li et al., 2022b) because PA can act as a crosslinker to form a hydrogel as well as serve as an adhesion site to glycosyl compounds in cell membranes. The hydrogel exhibited stronger adhesion strength to porcine skin with self-healing, injectability, and stronger mechanical properties than commercial fibrin glue, an indication of multiple functions by single-component networks. In addition, the hydrogel showed a faster hemostatic time of 30 s with a blood loss of 40 mg in an SD rat liver

puncture model than fibrin glue. Therefore, these hydrogels can be the first single-component HA-based TA for hemostasis and wound closure.

Fan et al. prepared dual-functionalized HA hydrogel TAs based on DO-conjugated maleic HA (DMHA) through the photocrosslinking of DMHA in situ for rapid hemostasis as shown in (Fig. 15) (Fan et al., 2023) because the introduction of acrylate and DO groups in the DMHA macromer endowed strong TA properties with rapid gelation behavior. Hydrogels with a high content of DO and acrylate groups induced red blood cell aggregation and platelet adhesion in vitro, although their properties were due to the high content of DO in the unoxidized state. In addition, the hydrogel exhibited superior hemostatic properties in a rat liver injury model compared to commercial products such as gauze and absorbable GE sponges. This is an indication of these hydrogel being promising candidates for hemorrhage control due to the multifunctional

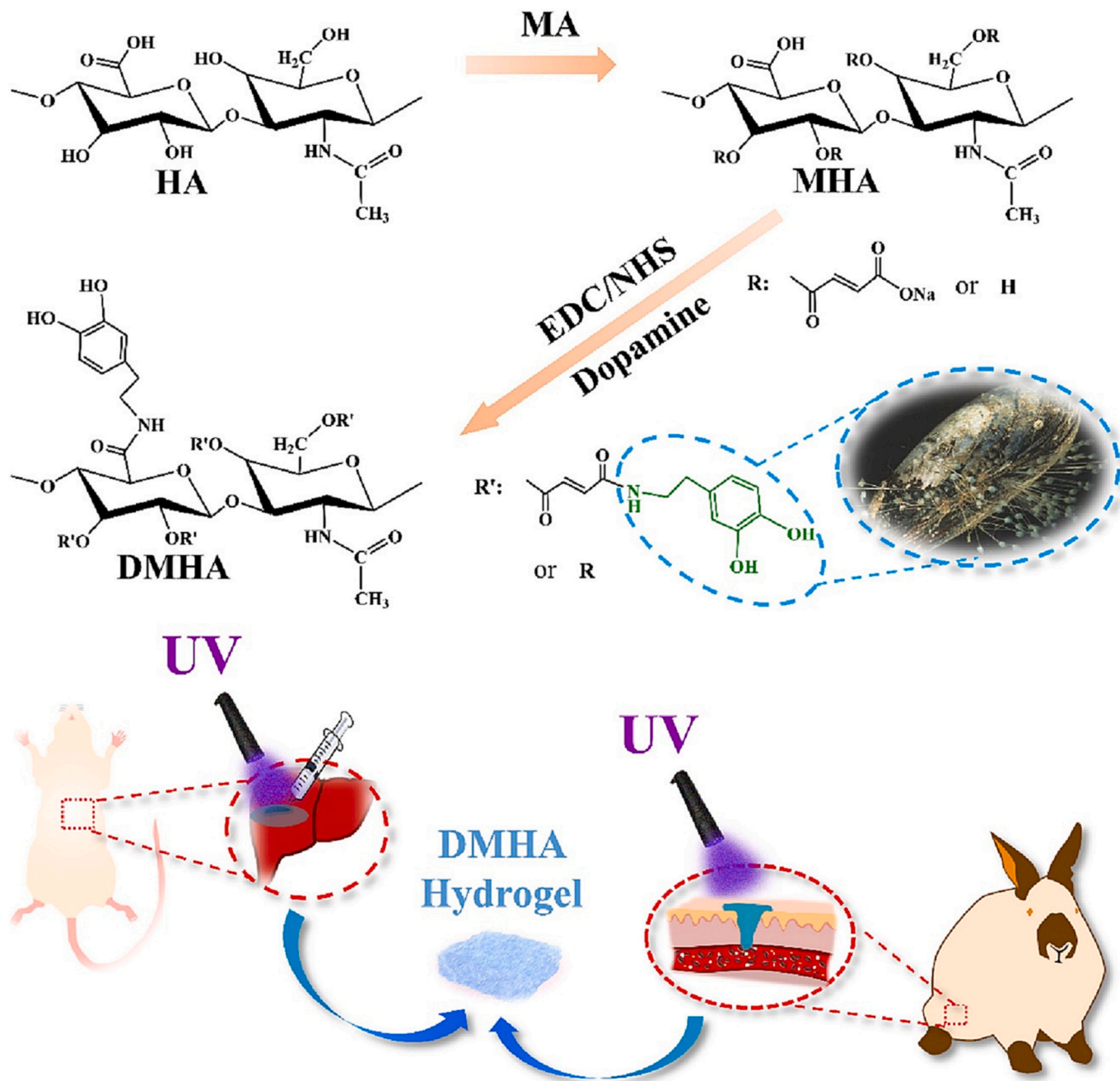


Fig. 15. Schematic illustrations of DMHA hydrogel adhesives for rapid hemostasis in vivo. Synthesis route and hydrogel formation in lesion area in situ by UV irradiation.

[Adapted from Fan et al., 2023 with permission from Elsevier.]

properties of TAs.

6.4.3.2. Wound healing. Zhang et al. prepared photo-crosslinking hydrogel TAs based on the photo-triggered S-nitrosylation coupling reaction of HA for oral mucosal wound healing (Zhang et al., 2021b) because the TA of the oral mucosal wound should be thin, elastic, and protective from disturbance by liquid rinsing, oral movement, and friction for more than 24 h. Gelation of this hydrogel occurred within 5 s because of the S-nitrosylation reaction. In addition, the hydrogel shortened oral mucosal defects in both rat and pig oral mucosa repair models, with tight adhesion to the wet surface and excellent elasticity. This is an indication of these hydrogel being promising candidates for the wound healing of oral mucosal defects using light-curing techniques.

Long et al. prepared injectable AGNPs and co-loaded DO-grafted HA/PA-grafted methylcellulose (MC) hydrogel TAs for chronic wound repair (Long et al., 2022) because these hydrogels have multifunctional properties, such as rapid gelation time, self-healing, strong tissue adhesiveness, and antioxidant and antibacterial properties. The hydrogel promoted cell proliferation and high antibacterial activity owing to the release of AG from the hydrogel according to the pH-/H₂O₂-responsive release mechanism. In addition, the hydrogel significantly accelerated wound repair in a diabetic bacteria-infected rat model owing to enhanced CO deposition. This is an indication of these hydrogel being promising candidates for the chronic wound dressings due to their multifunctional properties.

6.4.3.3. Bone formation. Choi et al. prepared HAP [or whitlockite (WKT)]- and bone morphogenetic protein-2 (BMP-2)-loaded pyrogallol (PG)-conjugated HA hydrogel TAs for bone formation (Choi et al., 2020) because HAP or WKT are osteoconductive inorganic particles, BMP-2 can promote bone formation, and the PG groups in PG-conjugated HA have a high binding affinity to the amine groups of the tissue (Lee, Rho, & Messersmith, 2009). The released HAP (or WKT) from the hybrid patch improved the mechanical properties and reinforced the structural properties, and the released BMP-2 significantly increased the expression of the osteogenic markers Runx2 and OPN compared to the cells treated with the control without BMP-2. In addition, the hybrid patches enhanced osteogenic differentiation of human stem cells in vitro and promoted new bone formation in critically sized calvarial bone defects in mice. This is an indication of these hydrogel being promising candidates for orthopedic applications due to the translational potential of phenolic TAs.

6.4.3.4. Maxillofacial tissue repair. Salzlechner et al. developed MA- and DO-conjugated HA hydrogel TAs for maxillofacial tissue repair (Salzlechner et al., 2020) because this adhesive hydrogel can be applied in a minimally invasive surgical procedure because of the quick gelation using surgical light, and human marrow stromal cells encapsulated within the hydrogel can be attached and survive upon oxidation of DO groups in the hydrogel. Gelation of the hydrogel occurred in less than 4 min with low degrees of DO upon irradiation using the photoinitiator Eosin Y. Additionally, the hydrogel bonded to the cut surfaces of a mouse's hind limb muscle and remained for 5 d, although in vivo assessments were not conducted. This is an indication of their use in minimally invasive procedures to foster maxillofacial tissue repair.

6.4.3.5. Spinal cord injury (SCI). Mu et al. prepared hypoxia-stimulated MSC-derived exosome-loaded adhesive peptide (PPFLMLLK-GSTR)-grafted HA hydrogel TAs for angiogenic therapy of SCI (Mu et al., 2022) because the adhesive peptide introduced into the hydrogel can bind to the integrin on loaded exosome membranes (Li et al., 2020a), and the exosomes obtained by hypoxia stimulation of MSCs can improve angiogenesis and functional motor restoration (Mu et al., 2022). The exosome-loaded hydrogel replenished the spinal cavity of rats with SCI, and the hypoxia-inducible factor 1- α content was significantly

increased in the endothelial cells surrounding the transplanted exosome-loaded hydrogel, indicating its potential in treating central nervous system trauma. This is an indication of these hydrogel being promising candidates for the treatment of central nervous system trauma due to the loaded stem cell-derived exosomes present in the TAs.

6.4.3.6. Corneal regeneration. Koivusalo et al. grafted DO moieties into hydrazone-crosslinked HA hydrogel TAs for corneal regeneration after loading of hASCs in the hydrogels and conjugation of thiolated CO IV to make tissue-like cellular compartmentalization in the implants (Koivusalo et al., 2019). The hASCs-loaded onto the hydrogel exhibited good proliferation and cell elongation. Moreover, compartmentalized hydrogel implants in a porcine corneal organ culture model exhibited excellent tissue adhesion, with over 90 % light transmittance over the entire visible spectrum. This is an indication of these hydrogel being promising candidates for the next generation of corneal regeneration due to the loaded stem cells present in the TAs.

6.4.3.7. Drug delivery system. Arunprasert et al. prepared ketoprofen drug-loaded CA-grafted poly (hydroxyethyl acrylate-co-itaconic acid) (CA-PHI)/HA composite TAs for transdermal drug delivery (TDD) (Arunprasert et al., 2022) because this pressure-sensitive adhesive patch can be applied to deliver a drug through the skin. The patches exhibited considerably greater adhesion ability to human skin with low toxicity compared with commercial patches because of the incorporated CA in CA-PH I, an indication of potential TDD systems for the delivery of a drug through the skin.

Mi et al. prepared engineered endothelium-derived exosomes (EC-EX^{mir-26a-5p}) and APY-loaded HA-based hydrogel TAs for fracture repair (Mi et al., 2022) because in situ gelation occurs by the reaction between aldehyde/quaternary ammonium-modified HA and hydrazide-modified HA, and the loaded EC-Exos^{mir-26a-5p} and APY 29 in the HA hydrogel are osteoblast/osteoclast and macrophage regulators, respectively. Cocktail therapy inhibited pro-inflammatory cytokines, promoted M2 polarization and osteogenic differentiation, and suppressed osteoclast differentiation in vitro. The hydrogel showed an enhanced pro-fracture repair effect in mice with femoral fractures. This is an indication of these hydrogel being promising candidates for fracture repair due to the cocktail therapy of exosome/drug delivery TAs.

He et al. prepared epigallocatechin-3-gallate (EGG)-loaded HA hydrogel TAs based on the phenylborate ester reaction of EGG, phenylboronic acid (PA)-modified MAHA, and MAGE by the photo-crosslinking for treatment of oxidative stress and inflammation (He et al., 2023) because the loaded EGG plays roles as an anti-inflammatory and antioxidative activity with the dynamic crosslinking agent. The hydrogel scavenged intracellular ROS and suppressed the expression of pro-inflammatory factors in vitro through the release of EGG from the EGG-loaded hydrogel due to the acid-responsive release of EGG, although in vivo assessments were not performed. This is an indication of these hydrogel being promising candidates for the alleviation of inflammatory disturbance due to them being EGG-loaded HA-based TAs.

6.4.3.8. Conductive wound dressing. Recently, Liang et al. prepared reduced graphene oxide (γ GO)-loaded conducting injectable DO-HA hydrogel TAs using an H₂O₂/HPR system for full-thickness skin repair (Liang et al., 2019), because the loaded γ GO in the hydrogel favors enhanced wound healing owing to the conductivity of γ GO (Guo, Finne-Wistrand, & Albertsson, 2011). The hydrogel significantly enhanced vascularization, improved granulation tissue thickness with CO deposition, and promoted wound closure compared to the commercial Tegaderm film in a mouse full-thickness wound model. This is an indication of these hydrogels being promising candidates for skin regeneration. This is because they are hemostatic conducting injectable HA-based TAs, which can control drug release and photothermal antibacterial activity.

6.4.3.9. Three-dimensional (3D) bioprinting for adhesive tissue engineering. 3D bioprinting as an additive biomanufacturing method can provide the scaffold fabrication of biological constructs according to pre-designed digital model (Murphy & Atala, 2014). Micro-extrusion bioprinting among conventional extrusion bioprinting systems has been the most used method for fabrication of scaffolds by squeezing out bioinks from a syringe nozzle. It can print at high cell densities and control cellular damages with less complex and cost-effectiveness although it has low printing speed and limited choice of extrudable bioinks (You, Eames, & Chen, 2017).

Chen et al. used embedded extrusion-based bioprinting method for fabrication of adhesive soft tissue engineering scaffolds to secure implants onto target tissue using a combination of DA-grafted MAHA- and MAGE-based bioinks (Chen et al., 2023a). The fabricated scaffolds exhibited strong adhesion property onto the adherend collagen substrate imitating the native tissue and under wet dynamic loading condition with maintenance of their structural fidelity, mechanical properties, and biocompatibility. This is an indication of these hybrid functionalized hydrogel bioinks being promising candidates for the translational applications although they did not perform in vivo study.

Jongprasitkul et al. prepared pH-sensitive TA hydrogels composed of gallic acid-grafted HA(GAHA) and MAHA for injection and 3D bioprinting (Jongprasitkul, Parihar, Turunen, & Kellomaki, 2023). The GAHA/MAHA blends have pH-dependent viscosity for improved injectability and printability in the precursor phase, and the GAHA/MAHA blends can be photo-crosslinked for creation of hydrogel with a complementary network of both GAHA and MAHA. The hydrogels exhibited sufficient printing quality and accuracy with enhanced viscoelastic and stable swelling properties compared to MAHA. Also, GAHA component provided tissue adhesion on chicken skins and porcine muscles, and antioxidant activity with pH tunability. This is an indication of these blended hydrogel bioinks being promising candidates for the printing on an infected wound site due to their tissue adhesiveness and dimensional stability in situ although they did not perform in vivo study.

A list of applications using HA-based TAs is shown in Table 4.

Table 4
A list of applications using HA-based TAs.

Category	Main components	In vivo model	Target tissue	Results	Reference
Hemostasis	3-Aminophenylboronic acid, hyaluronic acid	Rat	Skin	Fast hemostatic ability due to the phenylboronic acid as an adhesion site in cell membranes	(Fan et al., 2023)
	Dopamine, maleic anhydride, hyaluronic acid	Rat	Liver	Superior hemostatic property due to the fast crosslinking by dopamine and high content of acrylate groups	(Zhang et al., 2021b)
Wound healing	Methyl-ester-based o-nitrobenzyl sulfide, hyaluronic acid	Rat	Oral mucosa	Promotion of wound healing due to the S-nitrosylation by photoreaction	(Long et al., 2022)
	Dopamine, phenylboronic acid, methylcellulose, hyaluronic acid, Ag ⁺ , collagen	Rat	Skin	Accelerated wound repair due to the loaded Ag ⁺ and collagen	(Choi et al., 2020)
Bone formation	Hydroxyapatite, pyrogallol, bone morphogenetic protein-2, hyaluronic acid	Mouse	Bone	Promotion of new bone formation due to the osteoconductive properties by the hydroxyapatite and bone morphogenetic protein-2	(Lee et al., 2009)
Maxillofacial tissue repair	Dopamine, methacrylate, hyaluronic acid, marrow stromal cells	Non-treatment	Non-treatment	Fostering tissue adhesion and cell attachment due to the dopamine group and marrow stromal cells	(Mu et al., 2022)
Spinal cord injury	Exosome, adhesive peptide, hyaluronic acid	Rat	Spinal cord	Effective spinal cord regeneration due to the prominent angiogenesis and functional recovery by the loaded exosomes	(Li et al., 2020a)
Corneal regeneration	Dopamine, hydrazone, hyaluronic acid, laminin-derived peptide, collagen IV, human adipose-derived stem cells	Porcine	Eye	Displaying over 90 % light transmittance due to the loaded adipose-derived stem cells	(Arunprasert et al., 2022)
	Ketoprofen, dopamine, poly(hydroxyethyl acrylate-co-itaconic acid), hyaluronic acid	Pig	Skin	Greater adhesion ability to human skin due to the dopamine	(Mi et al., 2022)
Drug delivery system	Exosome, APY29, hydrazide hyaluronic acid	Mouse	Femoral fracture	Pro-fracture repair due to the loaded exosome and APY 29	(He et al., 2023)
	Epigallocatechin-3-gallate, phenylboronic acid, methacrylate, hyaluronic acid	Non-treatment	Non-treatment	Effective treatment of oxidative stress and inflammation due to the loaded epigallocatechin-3-gallate	(Liang et al., 2019)

6.4.4. Advantages and disadvantages

There are several advantages, such as a natural moisturizer with a high water-binding capacity due to the highly hydrophilic molecule, biocompatibility due to the finding in mammalian tissues, non-immunogenicity, and participation in cell-matrix interactions for providing instructive cell signaling (Collins & Birkinshaw, 2013). However, HA exhibits poor mechanical properties owing to its high swelling and rapid degradation. In addition, the degradation products of HA, in some cases, induce an inflammatory response in dendritic cells and macrophages (Tesar et al., 2006).

6.5. Clinically approved polysaccharide (PS)-based tissue adhesives (TAs)

The clinically approved PS-based TAs are listed in Table 5, although only a few PS-based TAs are clinically approved compared to synthetic polymer- and protein-based TAs.

7. Conclusion and perspectives

Sutures have been widely used to seal and close wounds because they are simple and rapidly applicable for manage wounds, although patients experience pain and discomfort under invasive techniques. Therefore, the development of new TAs is of great interest to scientists and industries because they can reduce surgery time and pain, prevent bleeding, and omit removal procedures. CS-based TAs are used as hemostatic agents, wound closure, bone regeneration, and drug delivery systems owing to their biocompatibility, biodegradability, antibacterial activity, and the possibility of various formulations and chemical modifications. However, it is not easy to control their physicochemical and biological properties owing to their different origins, molecular weights, and degrees of acetylation from chitin. AL-based TAs are used as hemostatic agents and wound dressings, as well as in bone and cartilage regeneration, drug delivery, bioelectronics, tendon healing, colon-targeting, and corneal regeneration owing to their biocompatibility, wound healing ability, good injectability, low toxicity, and good swelling behavior. They also rapidly adsorb wound exudates and create

Table 5

A list of clinically approved PS-based adhesives.

Company name (country name)	Trade name	Components	Clinic applications	Reference
HemCon Medical Technologies Inc. (USA)	ProChitogauze	Chitosan	Wound dressing for control of bleeding	(Bennett, 2017)
MedTrade Products Ltd. (UK)	Celox gauze	Chitosan	Wound dressing for control of bleeding	(Bennett, 2017)
Aspen Medical (USA)	Sorbsan	Alginate	Diabetic ulcers	(Bal-Ozturk et al., 2021)
Sealntis (Malaysia)	Seal-V	Alginate	Hemostasis in surgical reconstruction of blood vessels	(Nam & Mooney, 2021)
Genzyme Corporation (USA)	Seprafilm Adhesion Barrier	Hyaluronic acid and carboxymethyl-cellulose	Abdominal or pelvic laparotomy	(Diamond, Burns, Accomando, Mian, & Holmdahl, 2012)

cross-linkers. However, the G/M block ratio affects the physicochemical properties of AL, and ionically cross-linked AL can be easily dissolved in water. DE-based TAs are used for hemostasis, wound dressing, lung injury, bone regeneration, periodontal disease, infarcted myocardium, and bioelectronics due to their biocompatibility, degradability, injectability, and low toxicity because of the rapid in situ gelation and easy application of hemostatic TA using a simple lyophilized DE sponge. However, the degradation of ODE TH is rapid, and a large amount of TA must be used to obtain adequate adhesion properties. HA-based TAs are used as hemostatic agents in wound healing, bone formation, maxillo-facial tissue repair, spinal cord injury, corneal regeneration, drug delivery systems, and conductive wound dressings owing to their high water-binding capacity, biocompatibility, non-immunogenicity, angiogenesis, and provision of instructive cell signaling. However, they have poor mechanical properties, and their degradation products induce inflammatory responses in immune cells. Overall, CS, AL, DE, and HA have been shown to be biocompatible, injectable, non-immunogenic, and low-toxic. CS, DE, and HA, except AL, are degradable. The origins of CS and AL affect their physicochemical and biological properties. Among some of the inherent properties of PS-based TAs, such as, CS being an antibacterial agent, AL being a wound-healing agent, DE being a hemostasis agent, and HA being an angiogenesis are appropriate platforms for tissue adhesive formulations. The schematic abstract of PS-based TAs is also shown in the Graphical abstract.

Currently, a significant gap exists between studies on PS-based TAs and those on clinically approved products. To address this, it is necessary to design TAs with a deep understanding of the tissue target surface properties and biomaterials, including possible adhesion mechanisms and their clinical limitations. The physicochemical properties, tissue responses, and long-term performance of TAs should be considered while monitoring the long-term efficacy of the implanted adhesives. Additionally, the fabrication of stimuli-responsive TAs using pH, light, temperature, magnetic, and conductive responsive adhesives for drug delivery is a very critical shortcoming. Furthermore, an understanding of the developmental pathways and regulations in clinical trials should be considered. Moreover, close collaboration between materials researchers, molecular scientists, and clinicians is required. Furthermore, next-generation TAs using biomimetic materials, such as mussels, geckos, slugs, and octopuses, are expected to provide sufficient tissue adhesion with multifunctional properties, although the economic limitations should be considered.

CRediT authorship contribution statement

Gi-Yeon Han: Conceptualization, Data curation, Writing – original draft, Writing – review & editing. **Ho-Wook Kwack:** Data curation, Writing – original draft. **Yo-Han Kim:** Writing – review & editing, Writing – original draft. **Yeon Ho Je:** Conceptualization, Writing – review & editing. **Hyun-Joong Kim:** Conceptualization, Data curation, Project administration, Writing – review & editing. **Chong-Su Cho:** Conceptualization, Data curation, Project administration, Writing – original draft, Writing – review & editing.

Declaration of competing interest

The authors declare that they have no known competing financial interests or personal relationships that could have appeared to influence the work reported in this paper.

Data availability

Data will be made available on request.

Acknowledgments

This research was supported by Basic Science Research Program through the National Research Foundation of Korea (NRF) funded by the Ministry of Education (NRF2020R111A1A01053275). Also, this work was carried out with the support of “Cooperative Research Program for Agriculture Science and Technology Development (Project No. PJ01497803)” Rural Development Administration, Republic of Korea.

Ethical statement

There are no animal experiments carried out for this article.

References

- Adams, J. C. (2023). Passing the post: Roles of posttranslational modifications in the form and function of extracellular matrix. *American Journal of Physiology-Cell Physiology*, 324(5), C1179–C1197.
- Aderibigbe, B. A., & Buyana, B. (2018). Alginate in wound dressings. *Pharmaceutics*, 10(2), 42.
- Agüero, L., Zaldivar-Silva, D., Peña, L., & Dias, M. L. (2017). Alginate microparticles as oral colon drug delivery device: A review. *Carbohydrate Polymers*, 168, 32–43.
- An, Y.-H., et al. (2018). Enzyme-mediated tissue adhesive hydrogels for meniscus repair. *International Journal of Biological Macromolecules*, 110, 479–487.
- Arunprasert, K., et al. (2022). Mussel-inspired poly(hydroxyethyl acrylate-co-itaconic acid)-catechol/hyaluronic acid drug-in-adhesive patches for transdermal delivery of ketoprofen. *International Journal of Pharmacology*, 629, Article 122362.
- Auriemma, M., et al. (2015). Blending poly (3-hydroxybutyrate) with tannic acid: Influence of a polyphenolic natural additive on the rheological and thermal behavior. *European Polymer Journal*, 63, 123–131.
- Baek, J., Kim, S., Son, I., Choi, S. H., & Kim, B. S. (2021). Hydrolysis-driven viscoelastic transition in triblock copolyether hydrogels with acetal pendants. *ACS Macro Letters*, 10(8), 1080–1087.
- Bai, Z., et al. (2018). Tough and tissue-adhesive polyacrylamide/collagen hydrogel with dopamine-grafted oxidized sodium alginate as crosslinker for cutaneous wound healing. *RSC Advances*, 8(73), 42123–42132.
- Bakhtyar, N., Jeschke, M. G., Herer, E., Sheikholeslam, M., & Amini-Nik, S. (2018). Exosomes from acellular Wharton's jelly of the human umbilical cord promotes skin wound healing. *Stem Cell Research & Therapy*, 9(1), 193.
- Balakrishnan, B., Payanam, U., Laurent, A., Wassef, M., & Jayakrishnan, A. (2021). Efficacy evaluation of anin situ forming tissue adhesive hydrogel as sealant for lung and vascular injury. *Biomedical Materials*, 16(4).
- Bal-Ozturk, A., et al. (2021). Tissue adhesives: From research to clinical translation. *Nano Today*, 36.
- Banerjee, A., Chatterjee, K., & Madras, G. (2014). Enzymatic degradation of polymers: A brief review. *Materials Science and Technology*, 30(5), 567–573.
- Bao, Z., Gao, M., Sun, Y., Nian, R., & Xian, M. (2020). The recent progress of tissue adhesives in design strategies, adhesive mechanism and applications. *Materials Science and Engineering: C*, 111, Article 110796.
- Bennett, B. L. (2017). Bleeding control using hemostatic dressings: Lessons learned. *Wilderness & Environmental Medicine*, 28(2), S39–S49.

- Berg, I., et al. (2021). Factor XIII cross-linked adhesive chitosan hydrogels. *ACS Biomaterials Science & Engineering*, 7(6), 2198–2203.
- Bermejo-Velasco, D., et al. (2019). First aldol cross-linked hyaluronic acid hydrogel: Fast and hydrolytically stable hydrogel with tissue adhesive properties. *ACS Applied Materials & Interfaces*, 11(41), 38232–38239.
- Bertsch, P., Diba, M., Mooney, D. J., & Leeuwenburgh, S. C. (2022). Self-healing injectable hydrogels for tissue regeneration. *Chemical Reviews*, 123(2), 834–873.
- Bhagat, V., & Becker, M. L. (2017). Degradable adhesives for surgery and tissue engineering. *Biomacromolecules*, 18(10), 3009–3039.
- Bhatia, S. K., Arthur, S. D., Chenault, H. K., Figuly, G. D., & Kodokian, G. K. (2007). Polysaccharide-based tissue adhesives for sealing corneal incisions. *Current Eye Research*, 32(12), 1045–1050.
- Borie, E., et al. (2019). Oral applications of cyanoacrylate adhesives: A literature review. *BioMed Research International*, 2019.
- Buldak, L., et al. (2014). Metformin affects macrophages' phenotype and improves the activity of glutathione peroxidase, superoxide dismutase, catalase and decreases malondialdehyde concentration in a partially AMPK-independent manner in LPS-stimulated human monocytes/macrophages. *Pharmacological Reports*, 66(3), 418–429.
- Chen, G., et al. (2018). Bioinspired multifunctional hybrid hydrogel promotes wound healing. *Advanced Functional Materials*, 28(33).
- Chen, Q., et al. (2019). Electrospun chitosan/PVA/bioglase nanofibrous membrane with spatially designed structure for accelerating chronic wound healing. *Materials Science and Engineering: C*, 105, Article 110083.
- Chen, S., et al. (2023a). Extrusion-based 3D bioprinting of adhesive tissue engineering scaffolds using hybrid functionalized hydrogel bioinks. *Advanced Biology*, 7(7), Article e2300124.
- Chen, X., Yuk, H., Wu, J., Nabzdyk, C. S., & Zhao, X. (2020). Instant tough bioadhesive with triggerable benign detachment. *Proceedings of the National Academy of Sciences of the United States of America*, 117(27), 15497–15503.
- Chen, X., et al. (2023b). Injectable dopamine-polysaccharide in situ composite hydrogels with enhanced adhesiveness. *ACS Biomaterials Science & Engineering*, 9(1), 427–436.
- Chen, Z., et al. (2021). An injectable anti-microbial and adhesive hydrogel for the effective noncompressible visceral hemostasis and wound repair. *Materials Science and Engineering: C*, 129, Article 112422.
- Chen, Z., et al. (2023c). A triple-network carboxymethyl chitosan-based hydrogel for hemostasis of incompressible bleeding on wet wound surfaces. *Carbohydrate Polymers*, 303, Article 120434.
- Choi, S., et al. (2020). Osteoconductive hybrid hyaluronic acid hydrogel patch for effective bone formation. *Journal of Controlled Release*, 327, 571–583.
- Choi, Y., Kang, K., Son, D., & Shin, M. (2022). Molecular rationale for the design of instantaneous, strain-tolerant polymeric adhesive in a stretchable underwater human-machine interface. *ACS Nano*, 16(11), 1368–1380.
- Cintron-Cruz, J. A., et al. (2022). Rapid ultrathin topological tissue adhesives. *Advanced Materials*, 34(35), Article e2205567.
- Clegg, D. O., et al. (2006). Glucosamine, chondroitin sulfate, and the two in combination for painful knee osteoarthritis. *New England Journal of Medicine*, 354(8), 795–808.
- Collins, M. N., & Birkinshaw, C. (2013). Hyaluronic acid based scaffolds for tissue engineering—A review. *Carbohydrate Polymers*, 92(2), 1262–1279.
- Cui, C., et al. (2019). Water-triggered hyperbranched polymer universal adhesives: From strong underwater adhesion to rapid sealing hemostasis. *Advanced Materials*, 31(49), Article e1905761.
- Dev, A., et al. (2010). Preparation of poly (lactic acid)/chitosan nanoparticles for anti-HIV drug delivery applications. *Carbohydrate Polymers*, 80(3), 833–838.
- Diamond, M. P., Burns, E. L., Accomando, B., Mian, S., & Holmdahl, L. (2012). Sefrafil[®] adhesion barrier: (2) A review of the clinical literature on intraabdominal use. *Gynecological Surgery*, 9(3), 247–257.
- Dicker, K. T., et al. (2014). Hyaluronan: A simple polysaccharide with diverse biological functions. *Acta Biomaterialia*, 10(4), 1558–1570.
- Douglas, T. E. L., et al. (2014). Enzymatic mineralization of gellan gum hydrogel for bone tissue-engineering applications and its enhancement by polydopamine. *Journal of Tissue Engineering and Regenerative Medicine*, 8(11), 906–918.
- Du, X., et al. (2019). Injectable hydrogel composed of hydrophobically modified chitosan/oxidized-dextran for wound healing. *Materials Science and Engineering: C*, 104, Article 109930.
- Du, X., et al. (2020a). An anti-infective hydrogel adhesive with non-swelling and robust mechanical properties for sutureless wound closure. *Journal of Materials Chemistry B*, 8(26), 5682–5693.
- Du, X., et al. (2020b). Anti-infective and pro-coagulant chitosan-based hydrogel tissue adhesive for sutureless wound closure. *Biomacromolecules*, 21(3), 1243–1253.
- Erdi, M., Sandler, A., & Kofinas, P. (2023). Polymer nanomaterials for use as adjuvant surgical tools. *Wiley Interdisciplinary Reviews: Nanomedicine and Nanobiotechnology*, 15(4), e1889.
- Fan, P., et al. (2023). Flexible dual-functionalized hyaluronic acid hydrogel adhesives formed in situ for rapid hemostasis. *Carbohydrate Polymers*, 313, Article 120854.
- Fang, F., Linstadt, R. T. H., Genin, G. M., Ahn, K., & Thomopoulos, S. (2022). Mechanically competent chitosan-based bioadhesive for tendon-to-bone repair. *Advanced Healthcare Materials*, 11(10), Article e2102344.
- Farasatkia, A., & Kharaziha, M. (2021). Robust and double-layer micro-patterned bioadhesive based on silk nanofibril/GelMA-alginate for stroma tissue engineering. *International Journal of Biological Macromolecules*, 183, 1013–1025.
- Feig, V. R., et al. (2021). Conducting polymer-based granular hydrogels for injectable 3D cell scaffolds. *Advanced Materials Technologies*, 6(6), Article 2100162.
- Frati, C., et al. (2020). Reinforced alginate/gelatin sponges functionalized by avidin/biotin-binding strategy: A novel cardiac patch. *Journal of Biomaterials Applications*, 34(7), 975–987.
- Freedman, B. R., et al. (2022). Enhanced tendon healing by a tough hydrogel with an adhesive side and high drug-loading capacity. *Nature Biomedical Engineering*, 6(10), 1167–1179.
- Gao, Y., et al. (2021). Hydrogel-mesh composite for wound closure. *Proceedings of the National Academy of Sciences*, 118(28).
- Gasek, N., et al. (2021). Development of alginate and gelatin-based pleural and tracheal sealants. *Acta Biomaterialia*, 131, 222–235.
- Ghasemzadeh Rahbardar, M., & Hosseinzadeh, H. (2020). Effects of rosmarinic acid on nervous system disorders: An updated review. *Naunyn-Schmiedeberg's Archives of Pharmacology*, 393, 1779–1795.
- Goa, K. L., & Benfield, P. (1994). Hyaluronic acid. *Drugs*, 47(3), 536–566.
- Guo, B., Finne-Wistrand, A., & Albertsson, A.-C. (2011). Facile synthesis of degradable and electrically conductive polysaccharide hydrogels. *Biomacromolecules*, 12(7), 2601–2609.
- Guo, S., et al. (2022a). Injectable self-healing adhesive chitosan hydrogel with antioxidant, antibacterial, and hemostatic activities for rapid hemostasis and skin wound healing. *ACS Applied Materials & Interfaces*, 14(30), 34455–34469.
- Guo, Z., et al. (2022b). A Mg(2+)/polydopamine composite hydrogel for the acceleration of infected wound healing. *Bioactive Materials*, 15, 203–213.
- Han, G. Y., Hwang, S. K., Cho, K. H., Kim, H. J., & Cho, C. S. (2023). Progress of tissue adhesives based on proteins and synthetic polymers. *Biomaterials Research*, 27(1), 57.
- Han, G. Y., Park, J. Y., Lee, T. H., Yi, M. B., & Kim, H. J. (2022). Highly resilient dual-crosslinked hydrogel adhesives based on a dopamine-modified crosslinker. *ACS Applied Materials & Interfaces*, 14(32), 36304–36314.
- Han, W., et al. (2020). Biofilm-inspired adhesive and antibacterial hydrogel with tough tissue integration performance for sealing hemostasis and wound healing. *Bioactive Materials*, 5(4), 768–778.
- Haq, M. A., Su, Y., & Wang, D. (2017). Mechanical properties of PNIPAM based hydrogels: A review. *Materials Science and Engineering: C*, 70, 842–855.
- Hasani-Sadrabadi, M. M., et al. (2020). An engineered cell-laden adhesive hydrogel promotes craniofacial bone tissue regeneration in rats. *Science Translational Medicine*, 12(534), Article eaay6853.
- He, X. Y., et al. (2020). Mussel-inspired antimicrobial chitosan tissue adhesive rapidly activated in situ by H(2)O(2)/ascorbic acid for infected wound closure. *Carbohydrate Polymers*, 247, Article 116692.
- He, Z., et al. (2023). Injectable and tissue adhesive EGCG-laden hyaluronic acid hydrogel depot for treating oxidative stress and inflammation. *Carbohydrate Polymers*, 299, Article 120180.
- Hong, Y., et al. (2019). A strongly adhesive hemostatic hydrogel for the repair of arterial and heart bleeds. *Nature Communications*, 10(1), 2060.
- Hyon, W., et al. (2022). Elucidating the degradation mechanism of a self-degradable dextran-based medical adhesive. *Carbohydrate Polymers*, 278, Article 118949.
- Jain, R., & Wairkar, S. (2019). Recent developments and clinical applications of surgical glues: An overview. *International Journal of Biological Macromolecules*, 137, 95–106.
- Jongprasitkul, H., Parihar, V. S., Turunen, S., & Kellomaki, M. (2023). pH-responsive gallol-functionalized hyaluronic acid-based tissue adhesive hydrogels for injection and three-dimensional bioprinting. *ACS Applied Materials & Interfaces*, 15(28), 33972–33984.
- Ju, D. B., Lee, J. C., Hwang, S. K., Cho, C. S., & Kim, H. J. (2022). Progress of polysaccharide-contained polyurethanes for biomedical applications. *Tissue Engineering and Regenerative Medicine*, 19(5), 891–912.
- Jung, H. Y., Le Thi, P., HwangBo, K. H., Bae, J. W., & Park, K. D. (2021). Tunable and high tissue adhesive properties of injectable chitosan based hydrogels through polymer architecture modulation. *Carbohydrate Polymers*, 261, Article 117810.
- Kendall, K. (1975). Thin-film peeling—the elastic term. *Journal of Physics D: Applied Physics*, 8(13), 1449.
- Khor, E., & Lim, L. Y. (2003). Implantable applications of chitin and chitosan. *Biomaterials*, 24(13), 2339–2349.
- Kim, C.-G., et al. (2023a). Enhancement of immune responses elicited by nanovaccines through a cross-presentation pathway. *Tissue Engineering and Regenerative Medicine*, 20(3), 355–370.
- Kim, I.-Y., et al. (2008). Chitosan and its derivatives for tissue engineering applications. *Biotechnology Advances*, 26(1), 1–21.
- Kim, M. K., et al. (2018a). Tumor-suppressing miR-141 gene complex-loaded tissue-adhesive glue for the locoregional treatment of hepatocellular carcinoma. *Theranostics*, 8(14), 3891–3901.
- Kim, S., Choi, H., Son, D., & Shin, M. (2023b). Conductive and adhesive granular alginate hydrogels for on-tissue writable bioelectronics. *Gels*, 9(2).
- Kim, S., & Jung, S. (2020). Biocompatible and self-recoverable succinoglycan dialdehyde-crosslinked alginate hydrogels for pH-controlled drug delivery. *Carbohydrate Polymers*, 250, Article 116934.
- Kim, S. H., et al. (2018b). Enzyme-mediated tissue adhesive hydrogels for meniscus repair. *International Journal of Biological Macromolecules*, 110, 479–487.
- Kim, S. H., et al. (2018c). Tissue adhesive, rapid forming, and sprayable ECM hydrogel via recombinant tyrosinase crosslinking. *Biomaterials*, 178, 401–412.
- Kim, Y., Hu, Y., Jeong, J. P., & Jung, S. (2022). Injectable, self-healable and adhesive hydrogels using oxidized Succinoglycan/chitosan for pH-responsive drug delivery. *Carbohydrate Polymers*, 284, Article 119195.
- Koh, E., et al. (2023). Controlled delivery of corticosteroids using tunable tough adhesives. *Advanced Healthcare Materials*, 12(3), Article e2201000.
- Koivusalo, L., et al. (2019). Tissue adhesive hyaluronic acid hydrogels for sutureless stem cell delivery and regeneration of corneal epithelium and stroma. *Biomaterials*, 225, Article 119516.
- Lee, D.-H., & Bhang, S. H. (2023). Development of hetero-cell type spheroids via core-shell strategy for enhanced wound healing effect of human adipose-derived stem cells. *Tissue Engineering and Regenerative Medicine*, 1–11.

- Lee, H., Rho, J., & Messersmith, P. B. (2009). Facile conjugation of biomolecules onto surfaces via mussel adhesive protein inspired coatings. *Advanced Materials*, 21(4), 431–434.
- Lee, M., Wang, C. H., & Yeo, E. (2013). Effects of adherend thickness and taper on adhesive bond strength measured by portable pull-off tests. *International Journal of Adhesion and Adhesives*, 44, 259–268.
- Li, J., et al. (2017). Tough adhesives for diverse wet surfaces. *Science*, 357(6349), 378–381.
- Li, J., et al. (2018). Tough composite hydrogels with high loading and local release of biological drugs. *Advanced Healthcare Materials*, 7(9), Article 1701393.
- Li, J., et al. (2022a). Emerging biopolymer-based bioadhesives. *Macromolecular Bioscience*, 22(2), Article 2100340.
- Li, L., et al. (2020a). Transplantation of human mesenchymal stem-cell-derived exosomes immobilized in an adhesive hydrogel for effective treatment of spinal cord injury. *Nano Letters*, 20(6), 4298–4305.
- Li, M., Zhang, Z., Liang, Y., He, J., & Guo, B. (2020b). Multifunctional tissue-adhesive cryogel wound dressing for rapid nonpressing surface hemorrhage and wound repair. *ACS Applied Materials & Interfaces*, 12(32), 35856–35872.
- Li, M., et al. (2022b). Single-component hyaluronic acid hydrogel adhesive based on phenylboronic ester bonds for hemostasis and wound closure. *Carbohydrate Polymers*, 296, Article 119953.
- Li, W., et al. (2019). Tough bonding, on-demand debonding, and facile rebonding between hydrogels and diverse metal surfaces. *Advanced Materials*, 31(48), Article 1904732.
- Liang, Y., Xu, H., Li, Z., Zhangji, A., & Guo, B. (2022). Bioinspired injectable self-healing hydrogel sealant with fault-tolerant and repeated thermo-responsive adhesion for sutureless post-wound-closure and wound healing. *Nano-Micro Letters*, 14(1), 185.
- Liang, Y., et al. (2019). Adhesive hemostatic conducting injectable composite hydrogels with sustained drug release and photothermal antibacterial activity to promote full-thickness skin regeneration during wound healing. *Small*, 15(12), Article e1900046.
- Lin, X., Lv, J., Wang, D., & Liu, K. (2023). Injectable adhesive carboxymethyl chitosan-based hydrogels with self-mending and antimicrobial features for the potential management of periodontal diseases. *RSC Advances*, 13(18), 11903–11911.
- Liu, C., et al. (2019). A highly efficient, in situ wet-adhesive dextran derivative sponge for rapid hemostasis. *Biomaterials*, 205, 23–37.
- Liu, H., et al. (2021). Colon-targeted adhesive hydrogel microsphere for regulation of gut immunity and flora. *Advanced Science*, 8(18), Article e2101619.
- Liu, Y., et al. (2020). ZIF-8-modified multifunctional bone-adhesive hydrogels promoting angiogenesis and osteogenesis for bone regeneration. *ACS Applied Materials & Interfaces*, 12(33), 36978–36995.
- Lo Presti, M., Rizzo, G., Farinola, G. M., & Omenetto, F. G. (2021). Bioinspired biomaterial composite for all-water-based high-performance adhesives. *Advanced Science*, 8(16), Article 2004786.
- Loh, E. Y. X., et al. (2018). Development of a bacterial cellulose-based hydrogel cell carrier containing keratinocytes and fibroblasts for full-thickness wound healing. *Scientific Reports*, 8(1), 2875.
- Long, L., et al. (2022). Injectable multifunctional hyaluronic acid/methylcellulose hydrogels for chronic wounds repairing. *Carbohydrate Polymers*, 289, Article 119456.
- Lu, M., Liu, Y., Huang, Y. C., Huang, C. J., & Tsai, W. B. (2018). Fabrication of photocrosslinkable glycol chitosan hydrogel as a tissue adhesive. *Carbohydrate Polymers*, 181, 668–674.
- Lu, Q., et al. (2013). Nanomechanics of cation- π interactions in aqueous solution. *Angewandte Chemie*, 125(14), 4036–4040.
- Luo, L.-J., Lai, J.-Y., Chou, S.-F., Hsueh, Y.-J., & Ma, D. H.-K. (2018). Development of gelatin/ascorbic acid cryogels for potential use in corneal stromal tissue engineering. *Acta Biomaterialia*, 65, 123–136.
- Lynn, A. D., Kyriakides, T. R., & Bryant, S. J. (2010). Characterization of the in vitro macrophage response and in vivo host response to poly(ethylene glycol)-based hydrogels. *Journal of Biomedical Materials Research Part A*, 93(3), 941–953.
- Ma, Y., et al. (2018). Remote control over underwater dynamic attachment/detachment and locomotion. *Advanced Materials*, 30(30), Article e1801595.
- Ma, Y., et al. (2020). Liquid bandage harvests robust adhesive, hemostatic, and antibacterial performances as a first-aid tissue adhesive. *Advanced Functional Materials*, 30(39), Article 2001820.
- Maleki, M., et al. (2021). Multiple interactions between melatonin and non-coding RNAs in cancer biology. *Chemical Biology & Drug Design*, 98(3), 323–340.
- Marelli, B., et al. (2015). Newly identified interfibrillar collagen crosslinking suppresses cell proliferation and remodeling. *Biomaterials*, 54, 126–135.
- Mi, B., et al. (2022). Osteoblast/osteoclast and immune cocktail therapy of an exosome/drug delivery multifunctional hydrogel accelerates fracture repair. *ACS Nano*, 16(1), 771–782.
- Montazerian, H., et al. (2022). Bio-macromolecular design roadmap towards tough bioadhesives. *Chemical Society Reviews*, 51, 9127–9173.
- Moon, Y. J., et al. (2021). Beta-cyclodextrin/triclosan complex-grafted methacrylated glycol chitosan hydrogel by photocrosslinking via visible light irradiation for a tissue bio-adhesive. *International Journal of Molecular Sciences*, 22(2).
- Mu, J., et al. (2022). Hypoxia-stimulated mesenchymal stem cell-derived exosomes loaded by adhesive hydrogel for effective angiogenic treatment of spinal cord injury. *Biomaterials Science*, 10(7), 1803–1811.
- Munoz Taboada, G., Dosta, P., Edelman, E. R., & Artzi, N. (2022). Sprayable hydrogel for instant sealing of vascular anastomosis. *Advanced Materials*, 34(43), Article e2203087.
- Murphy, S. V., & Atala, A. (2014). 3D bioprinting of tissues and organs. *Nature Biotechnology*, 32(8), 773–785.
- Muzzarelli, R. A. (2009). Chitins and chitosans for the repair of wounded skin, nerve, cartilage and bone. *Carbohydrate Polymers*, 76(2), 167–182.
- Nam, S., & Mooney, D. (2021). Polymeric tissue adhesives. *Chemical Reviews*, 121(18), 11336–11384.
- Necas, J., Bartosikova, L., Brauner, P., & Kolar, J. (2008). Hyaluronic acid (hyaluronan): A review. *Veterinárni Medicína*, 53(8), 397–411.
- O'Rourke, R. D., et al. (2017). Addressing unmet clinical needs with UV bioadhesives. *Biomacromolecules*, 18(3), 674–682.
- Ozturk, E., et al. (2020). Tyrosinase-crosslinked, tissue adhesive and biomimetic alginate sulfate hydrogels for cartilage repair. *Biomedical Materials*, 15(4), Article 045019.
- Pandey, N., et al. (2018). Biodegradable nanoparticles enhanced adhesiveness of mussel-like hydrogels at tissue interface. *Advanced Healthcare Materials*, 7(7), Article e1701069.
- Pandey, N., et al. (2022). Polydopamine nanoparticles and hyaluronic acid hydrogels for mussel-inspired tissue adhesive nanocomposites. *Biomaterials Advances*, 134, Article 112589.
- Pang, J., et al. (2020). Mechanically and functionally strengthened tissue adhesive of chitin whisker complexed chitosan/dextran derivatives based hydrogel. *Carbohydrate Polymers*, 237, Article 116138.
- Park, E., Lee, J., Huh, K. M., Lee, S. H., & Lee, H. (2019). Toxicity-attenuated glycol chitosan adhesive inspired by mussel adhesion mechanisms. *Advanced Healthcare Materials*, 8(14), Article e1900275.
- Park, J., Kim, Y., Chun, B., & Seo, J. (2021). Rational engineering and applications of functional bioadhesives in biomedical engineering. *Biotechnology Journal*, 16(12), Article 2100231.
- Patil, N., Falentin-Daudré, C., Jérôme, C., & Detrembleur, C. (2015). Mussel-inspired protein-repelling ambivalent block copolymers: Controlled synthesis and characterization. *Polymer Chemistry*, 6(15), 2919–2933.
- Peng, X., et al. (2019). IO4-stimulated crosslinking of catechol-conjugated hydroxyethyl chitosan as a tissue adhesive. *Journal of Biomedical Materials Research Part B*, 107(3), 582–593.
- Peng, Z., et al. (2023). Tough, adhesive biomimetic hyaluronic acid methacryloyl hydrogels for effective wound healing. *Frontiers in Bioengineering and Biotechnology*, 11, Article 1222088.
- Perkucin, I., Lau, K. S. K., Morshead, C. M., & Naguib, H. E. (2022). Bio-inspired conductive adhesive based on calcium-free alginate hydrogels for bioelectronic interfaces. *Biomedical Materials*, 18(1).
- Pinnarati, R., Bhuiyan, M. S. A., Meyers, K., Rajachar, R. M., & Lee, B. P. (2019). Multifunctional biomedical adhesives. *Advanced Healthcare Materials*, 8(11), Article 1801568.
- Qiu, H., et al. (2023). A lubricant and adhesive hydrogel cross-linked from hyaluronic acid and chitosan for articular cartilage regeneration. *International Journal of Biological Macromolecules*, 243, Article 125249.
- Ramsden, C. A., & Riley, P. A. (2014). Tyrosinase: The four oxidation states of the active site and their relevance to enzymatic activation, oxidation and inactivation. *Bioorganic & Medicinal Chemistry*, 22(8), 2388–2395.
- Rao, K. M., Uthappa, U. T., Kim, H. J., & Han, S. S. (2023). Tissue adhesive, biocompatible, antioxidant, and antibacterial hydrogels based on tannic acid and fungal-derived carboxymethyl chitosan for wound-dressing applications. *Gels*, 9(5).
- Rao, K. M., et al. (2022). Tissue adhesive, self-healing, biocompatible, hemostatic, and antibacterial properties of fungal-derived carboxymethyl chitosan-polydopamine hydrogels. *Pharmaceutics*, 14(5).
- Redmond, R. W., & Kochevar, I. E. (2019). Medical applications of rose bengal-and riboflavin-photosensitized protein crosslinking. *Photochemistry and Photobiology*, 95(5), 1097–1115.
- Ruprai, H., et al. (2020). Porous chitosan adhesives with L-DOPA for enhanced photochemical tissue bonding. *Acta Biomaterialia*, 101, 314–326.
- de Sainte Claire, P. (2009). Degradation of PEO in the solid state: A theoretical kinetic model. *Macromolecules*, 42(10), 3469–3482.
- Salazar, P., Martín, M., & González-Mora, J. (2016). Polydopamine-modified surfaces in biosensor applications. In *Polymer science: Research advances, practical applications and educational aspects* (pp. 385–396).
- Salzlechner, C., et al. (2020). Adhesive hydrogels for maxillofacial tissue regeneration using minimally invasive procedures. *Advanced Healthcare Materials*, 9(4), Article e1901134.
- Samanta, S., et al. (2022). Interpenetrating gallol functionalized tissue adhesive hyaluronic acid hydrogel polarizes macrophages to an immunosuppressive phenotype. *Acta Biomaterialia*, 142, 36–48.
- Sanandiya, N. D., et al. (2019). Tunichrome-inspired pyrogallol functionalized chitosan for tissue adhesion and hemostasis. *Carbohydrate Polymers*, 208, 77–85.
- Sato, T., Aoyagi, T., Ebara, M., & Auzély-Velty, R. (2017). Catechol-modified hyaluronic acid: In situ-forming hydrogels by auto-oxidation of catechol or photo-oxidation using visible light. *Polymer Bulletin*, 74, 4069–4085.
- Scognamiglio, F., et al. (2016). Adhesive and sealant interfaces for general surgery applications. *Journal of Biomedical Materials Research Part B: Applied Biomaterials*, 104(3), 626–639.
- Shakir, M., Prashant, K., Keerti, J., & K. T. R., & NK, J. (2016). Mucoadhesion: A promising approach in drug delivery system. *Reactive and Functional Polymers*, 100, 151–172.
- Shaz, B. H., & Hillyer, C. D. (2013). *Transfusion medicine and hemostasis: Clinical and laboratory aspects*. Newnes.
- Shin, M., et al. (2017). Complete prevention of blood loss with self-sealing haemostatic needles. *Nature Materials*, 16(1), 147–152.
- Shirzaei Sani, E., et al. (2018). Engineering adhesive and antimicrobial hyaluronic acid/elastin-like polypeptide hybrid hydrogels for tissue engineering applications. *ACS Biomaterials Science & Engineering*, 4(7), 2528–2540.

- Shokrani, H., et al. (2022). Biomedical engineering of polysaccharide-based tissue adhesives: Recent advances and future direction. *Carbohydrate Polymers*, 295, Article 119787.
- Shou, Y., et al. (2020). Thermoresponsive chitosan/DOPA-based hydrogel as an injectable therapy approach for tissue-adhesion and hemostasis. *ACS Biomaterials Science & Engineering*, 6(6), 3619–3629.
- Siddiqi, K. S., Husen, A., & Rao, R. A. (2018). A review on biosynthesis of silver nanoparticles and their biocidal properties. *Journal of Nanobiotechnology*, 16(1), 1–28.
- Singh, B., et al. (2015). Attuning hydroxypropyl methylcellulose phthalate to oral delivery vehicle for effective and selective delivery of protein vaccine in ileum. *Biomaterials*, 59, 144–159.
- Song, F., et al. (2021). A mussel-inspired flexible chitosan-based bio-hydrogel as a tailored medical adhesive. *International Journal of Biological Macromolecules*, 189, 183–193.
- Steiner, C. A., Karaca, Z., Moore, B. J., Imshaug, M. C., & Pickens, G. (2017). Surgeries in hospital-based ambulatory surgery and hospital inpatient settings, 2014: statistical brief# 223. In *Healthcare cost and utilization project (HCUP) statistical briefs* (p. 5).
- Su, Q., Wei, D., Dai, W., Zhang, Y., & Xia, Z. (2019). Designing a castor oil-based polyurethane as bioadhesive. *Colloids and Surfaces B: Biointerfaces*, 181, 740–748.
- Suh, J. B., Gent, A. N., & Kelly, I. S. G. (2007). Shear of rubber tube springs. *International Journal of Non-Linear Mechanics*, 42(9), 1116–1126.
- Sun, W., et al. (2022). Mussel-inspired polysaccharide-based sponges for hemostasis and bacteria infected wound healing. *Carbohydrate Polymers*, 295, Article 119868.
- Sun, Y., Sun, F., Xu, W., & Qian, H. (2023). Engineered extracellular vesicles as a targeted delivery platform for precision therapy. *Tissue Engineering and Regenerative Medicine*, 20(2), 157–175.
- Suneetha, M., Rao, K. M., & Han, S. S. (2019). Mussel-inspired cell/tissue-adhesive, hemostatic hydrogels for tissue engineering applications. *ACS Omega*, 4(7), 12647–12656.
- Suneetha, M., Zo, S., Choi, S. M., & Han, S. S. (2023). Antibacterial, biocompatible, hemostatic, and tissue adhesive hydrogels based on fungal-derived carboxymethyl chitosan-reduced graphene oxide-polydopamine for wound healing applications. *International Journal of Biological Macromolecules*, 241, Article 124641.
- Tan, H., Chu, C. R., Payne, K. A., & Marra, K. G. (2009). Injectable in situ forming biodegradable chitosan-hyaluronic acid based hydrogels for cartilage tissue engineering. *Biomaterials*, 30(13), 2499–2506.
- Tang, J., Li, J., Vlassak, J. J., & Suo, Z. (2016). Adhesion between highly stretchable materials. *Soft Matter*, 12(4), 1093–1099.
- Tarafder, S., Park, G. Y., Felix, J., & Lee, C. H. (2020). Bioadhesives for musculoskeletal tissue regeneration. *Acta Biomaterialia*, 117, 77–92.
- Tesar, B., et al. (2006). The role of hyaluronan degradation products as innate alloimmune agonists. *American Journal of Transplantation*, 6(11), 2622–2635.
- Tian, K., Suo, Z., & Vlassak, J. J. (2020). Chemically coupled interfacial adhesion in multilayered printing of hydrogels and elastomers. *ACS Applied Materials & Interfaces*, 12(27), 31002–31009.
- Tobing, S. D., & Klein, A. (2001). Molecular parameters and their relation to the adhesive performance of acrylic pressure-sensitive adhesives. *Journal of Applied Polymer Science*, 79(12), 2230–2244.
- Tondera, C., et al. (2019). Highly conductive, stretchable, and cell-adhesive hydrogel by nanoclay doping. *Small*, 15(27), Article e1901406.
- Trujillo-de Santiago, G., et al. (2019). Ocular adhesives: Design, chemistry, crosslinking mechanisms, and applications. *Biomaterials*, 197, 345–367.
- Tsai, W. B., & Wang, M. C. (2005). Effects of an avidin-biotin binding system on chondrocyte adhesion and growth on biodegradable polymers. *Macromolecular Bioscience*, 5(3), 214–221.
- Vacanti, C. A. (2006). The history of tissue engineering. *Journal of Cellular and Molecular Medicine*, 10(3), 569–576.
- Varaprasad, K., Jayaramudu, T., Kanikireddy, V., Toro, C., & Sadiku, E. R. (2020). Alginate-based composite materials for wound dressing application: A mini review. *Carbohydrate Polymers*, 236, Article 116025.
- Wang, B., et al. (2021). Mussel-inspired bisphosphonated injectable nanocomposite hydrogels with adhesive, self-healing, and osteogenic properties for bone regeneration. *ACS Applied Materials & Interfaces*, 13(28), 32673–32689.
- Wang, H., et al. (2023). An integrally formed janus hydrogel for robust wet-tissue adhesive and anti-postoperative adhesion. *Advanced Materials*, 35(23), Article e2300394.
- Wang, L., et al. (2022a). Targeting polysaccharides such as chitosan, cellulose, alginate and starch for designing hemostatic dressings. *Carbohydrate Polymers*, 291, Article 119574.
- Wang, S., et al. (2022b). A double-network strategy for the tough tissue adhesion of hydrogels with long-term stability under physiological environment. *Soft Matter*, 18(33), 6192–6199.
- Wang, X., et al. (2022c). Tough wet adhesion of hydrogen-bond-based hydrogel with on-demand debonding and efficient hemostasis. *ACS Applied Materials & Interfaces*, 14(31), 36166–36177.
- Wang, X., et al. (2022d). The biocompatibility of multi-source stem cells and gelatin-carboxymethyl chitosan-sodium alginate hybrid biomaterials. *Tissue Engineering and Regenerative Medicine*, 19(3), 491–503.
- Wang, Y., Yang, X., Nian, G., & Suo, Z. (2020). Strength and toughness of adhesion of soft materials measured in lap shear. *Journal of the Mechanics and Physics of Solids*, 143.
- Wei, Q., et al. (2022). Photo-induced adhesive carboxymethyl chitosan-based hydrogels with antibacterial and antioxidant properties for accelerating wound healing. *Carbohydrate Polymers*, 278, Article 119000.
- Werner, S., Krieg, T., & Smola, H. (2007). Keratinocyte-fibroblast interactions in wound healing. *Journal of Investigative Dermatology*, 127(5), 998–1008.
- Wilchek, M., & Bayer, E. A. (1990). Applications of avidin-biotin technology: Literature survey. *Methods in Enzymology*, 184, 14–45.
- Wu, M., et al. (2023a). Strong tissue adhesive polyelectrolyte complex powders based on low molecular weight chitosan for acute hemorrhage control. *International Journal of Biological Macromolecules*, 248, Article 125755.
- Wu, S. J., Yuk, H., Wu, J., Nabzdyk, C. S., & Zhao, X. (2021). A multifunctional origami patch for minimally invasive tissue sealing. *Advanced Materials*, 33(11), Article e2007667.
- Wu, T., et al. (2023b). Wet adhesive hydrogel cardiac patch loaded with anti-oxidative, autophagy-regulating molecule capsules and MSCs for restoring infarcted myocardium. *Bioactive Materials*, 21, 20–31.
- Xing, Y., et al. (2021). Injectable hydrogel based on modified gelatin and sodium alginate for soft-tissue adhesive. *Frontiers in Chemistry*, 9, Article 744099.
- Yan, S., et al. (2018). Preparation of mussel-inspired injectable hydrogels based on dual-functionalized alginate with improved adhesive, self-healing, and mechanical properties. *Journal of Materials Chemistry B*, 6(40), 6377–6390.
- Yang, J. H., Shin, H. H., Kim, D., Ryu, J. H., & Jin, E. J. (2023). Adhesive ginsenoside compound K patches for cartilage tissue regeneration. *Regenerative Biomaterials*, 10, Article rbad077.
- Yang, K., et al. (2022). Urastretchable, self-healable, and tissue-adhesive hydrogel dressings involving nanoscale tannic acid/ferric ion complexes for combating bacterial infection and promoting wound healing. *ACS Applied Materials & Interfaces*, 14(38), 43010–43025.
- Yang, S. Y., et al. (2013). A bio-inspired swellable microneedle adhesive for mechanical interlocking with tissue. *Nature Communications*, 4(1), 1702.
- Yao, S., et al. (2022). Injectable dual-dynamic-bond cross-linked hydrogel for highly efficient infected diabetic wound healing. *Advanced Healthcare Materials*, 11(14), Article e2200516.
- Yi, H., et al. (2005). Biofabrication with chitosan. *Biomacromolecules*, 6(6), 2881–2894.
- Yin, Y., et al. (2023). Rosmarinic acid-grafted dextran/gelatin hydrogel as a wound dressing with improved properties: Strong tissue adhesion, antibacterial, antioxidant and anti-inflammatory. *Molecules*, 28(10).
- Ying, B., Chen, R. Z., Zuo, R., Li, J., & Liu, X. (2021). An anti-freezing, ambient-stable and highly stretchable ionic skin with strong surface adhesion for wearable sensing and soft robotics. *Advanced Functional Materials*, 31(42).
- You, F., Eames, B. F., & Chen, X. (2017). Application of extrusion-based hydrogel bioprinting for cartilage tissue engineering. *International Journal of Molecular Sciences*, 18(7).
- Yu, X., et al. (2012). Polyvalent choline phosphate as a universal biomembrane adhesive. *Nature Materials*, 11(5), 468–476.
- Yuk, H., et al. (2019). Dry double-sided tape for adhesion of wet tissues and devices. *Nature*, 575(7781), 169–174.
- Zaaba, N. F., & Jaafar, M. (2020). A review on degradation mechanisms of polylactic acid: Hydrolytic, photodegradative, microbial, and enzymatic degradation. *Polymer Engineering & Science*, 60(9), 2061–2075.
- Zhang, F. X., et al. (2021a). Injectable mussel-inspired highly adhesive hydrogel with exosomes for endogenous cell recruitment and cartilage defect regeneration. *Biomaterials*, 278, Article 121169.
- Zhang, W., et al. (2020). Catechol-functionalized hydrogels: Biomimetic design, adhesion mechanism, and biomedical applications. *Chemical Society Reviews*, 49(2), 433–464.
- Zhang, W., et al. (2021b). Promoting oral mucosal wound healing with a hydrogel adhesive based on a phototriggered *o*-nitrosylation coupling reaction. *Advanced Materials*, 33(48), Article e2105667.
- Zhang, Y., et al. (2022). In situ-formed adhesive hyaluronic acid hydrogel with prolonged amnion-derived conditioned medium release for diabetic wound repair. *Carbohydrate Polymers*, 276, Article 118752.
- Zhao, K., et al. (2023). Engineered bicomponent adhesives with instantaneous and superior adhesion performance for wound sealing and healing applications. *Advanced Functional Materials*, 33(38), 2303509.
- Zheng, Z., et al. (2020). Catechol modified quaternized chitosan enhanced wet adhesive and antibacterial properties of injectable thermo-sensitive hydrogel for wound healing. *Carbohydrate Polymers*, 249, Article 116826.
- Zhou, D., et al. (2020). Dopamine-modified hyaluronic acid hydrogel adhesives with fast-forming and high tissue adhesion. *ACS Applied Materials & Interfaces*, 12(16), 18225–18234.
- Zhou, Y., Kang, L., Yue, Z., Liu, X., & Wallace, G. G. (2020). Composite tissue adhesive containing catechol-modified hyaluronic acid and poly-L-lysine. *ACS Applied Bio Materials*, 3(1), 628–638.
- Zhu, S., et al. (2023a). Microenvironment responsive nanocomposite hydrogel with NIR photothermal therapy, vascularization and anti-inflammation for diabetic infected wound healing. *Bioactive Materials*, 26, 306–320.
- Zhu, Z., et al. (2023b). A choline phosphoryl-conjugated chitosan/oxidized dextran injectable self-healing hydrogel for improved hemostatic efficacy. *Biomacromolecules*, 24(2), 690–703.
- Zou, C. Y., et al. (2022). Multi-crosslinking hydrogels with robust bio-adhesion and pro-coagulant activity for first-aid hemostasis and infected wound healing. *Bioactive Materials*, 16, 388–402.
- Lu, M.-M., et al. (2018). Antibacterial and biodegradable tissue nano-adhesives for rapid wound closure. *International Journal of Nanomedicine*, 5849–5863.